Nato Advanced Research Workshop
Metallic Materials with High Structural Efficiency

Kiev September 7th – 13th 2003

Neutron and synchrotron non-destructive methods for the characterisation of materials for different applications

Franco Rustichelli

Department of Sciences Applied to Complex Systems, Polytechnic University of Marche – Ancona (Italy)

INFM - Istituto Nazionale per la Fisica della Materia Research Unit of Ancona

Report Documentation Page

Form Approved
OMB No. 0704-0188

1. REPORT DATE	2. REPORT TYPE	3. DATES COVERED
18 MAR 2004	**N/A**	**-**

4. TITLE AND SUBTITLE	
Neutron and synchrotron non-destructive methods for the characterisation of materials for different applications	5a. CONTRACT NUMBER
	5b. GRANT NUMBER
	5c. PROGRAM ELEMENT NUMBER
6. AUTHOR(S)	5d. PROJECT NUMBER
	5e. TASK NUMBER
	5f. WORK UNIT NUMBER
7. PERFORMING ORGANIZATION NAME(S) AND ADDRESS(ES) **Department of Sciences Applied to Complex Systems, Polytechnic University of Marche Ancona (Italy)**	8. PERFORMING ORGANIZATION REPORT NUMBER
9. SPONSORING/MONITORING AGENCY NAME(S) AND ADDRESS(ES)	10. SPONSOR/MONITOR'S ACRONYM(S)
	11. SPONSOR/MONITOR'S REPORT NUMBER(S)

12. DISTRIBUTION/AVAILABILITY STATEMENT
Approved for public release, distribution unlimited

13. SUPPLEMENTARY NOTES
See also ADM001672., The original document contains color images.

14. ABSTRACT

15. SUBJECT TERMS

16. SECURITY CLASSIFICATION OF:			17. LIMITATION OF ABSTRACT	18. NUMBER OF PAGES	19a. NAME OF RESPONSIBLE PERSON
a. REPORT	b. ABSTRACT	c. THIS PAGE			
NATO/unclassified	**unclassified**	**unclassified**	**UU**	**55**	

Standard Form 298 (Rev. 8-98)
Prescribed by ANSI Std Z39-18

MMCs mechanical properties

TOUGHNESS

HARDNESS

DUCTILITY

MMCs replace
steel and cast iron
in automotive components

STRENGTH

LIGHT WEIGHT

Ceramic
Reinforcement

Metal Matrix

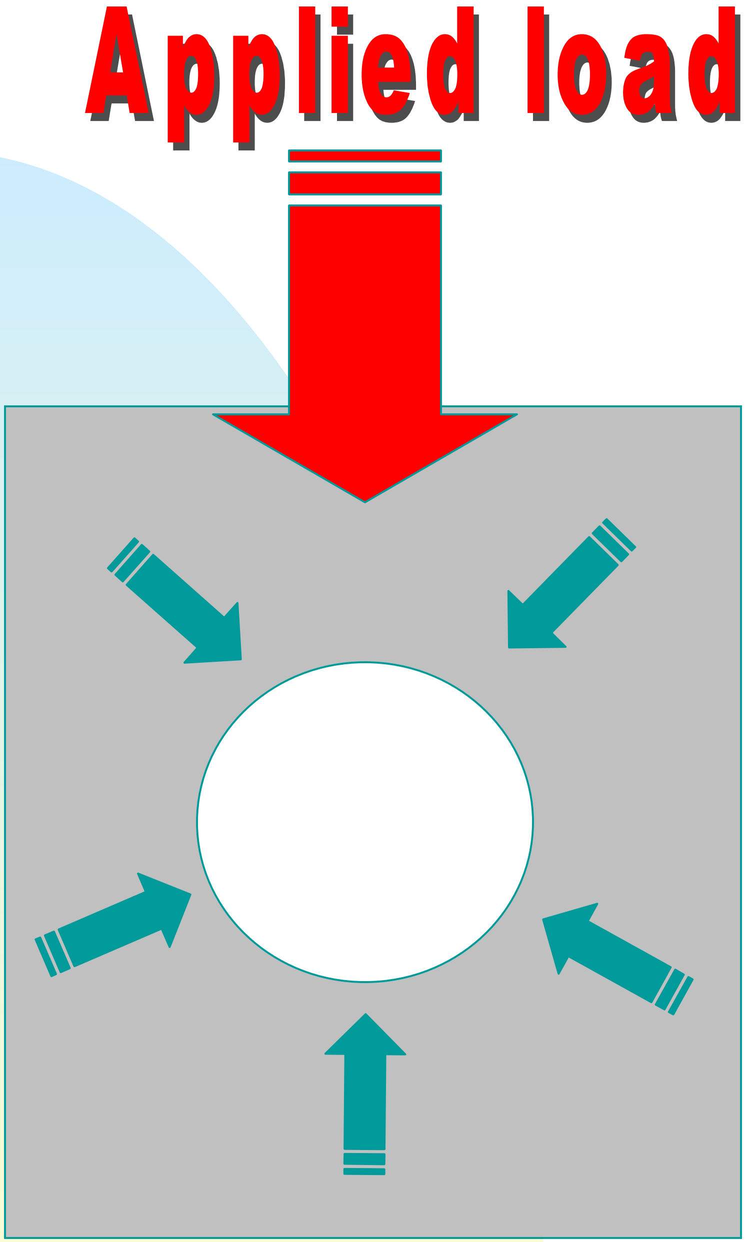

Load transfer

$$(1-f)\langle\sigma_M\rangle + f\langle\sigma_I\rangle = \sigma_A$$

- **Volume fraction (f);**
- **Reinforcement shape;**
- **Reinforcement orientation;**
- **Elastic properties of both phases.**

Large reinforcement size

High applied/residual stress

Particle clustering

Nucleation of precipitates

⟺

Formation of voids

Crack initiation

Fracture

Ductile fracture:

- after high plastic deformation ⇨ Excess of internal stress

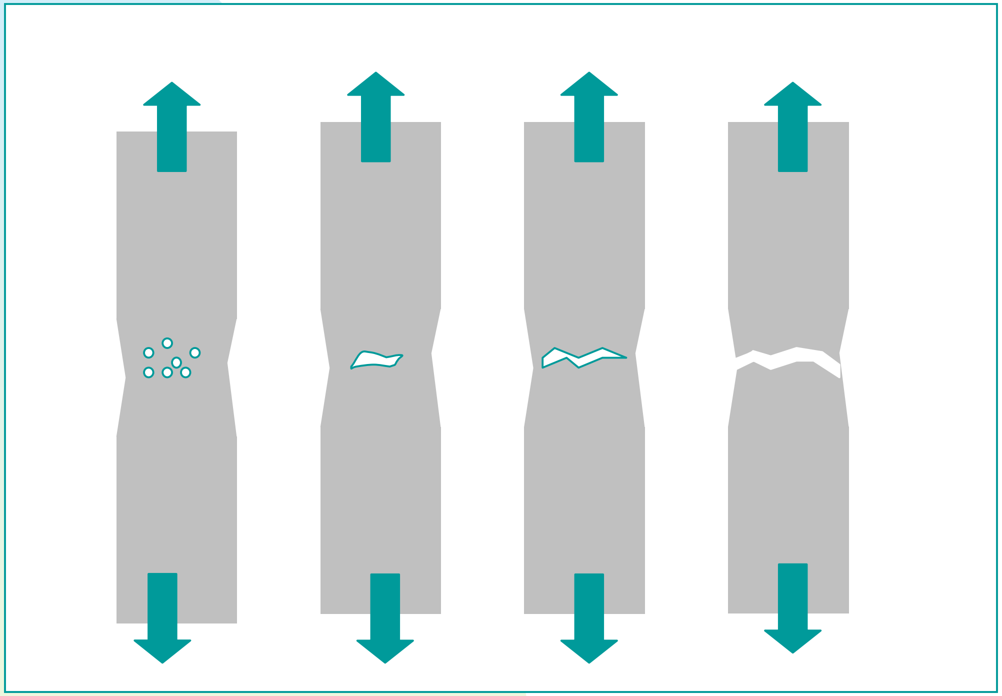

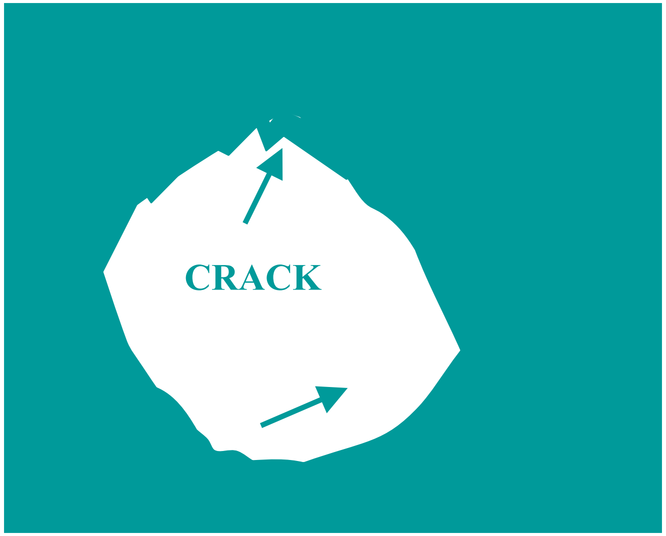

Internal Stress Analysis

before/after thermal/mechanical treatments

Brake Drum (AA359 + 20 vol. % SiCp)

3 identical brake drums → Die-casting → T6 heat treatment

Disamatic low pressure sand mould casting

Solubilization: 560°C x 2 hours;

Quenching: H_2O at 20°C;

Aging: 177°C x 10 hours.

1) as-cast brake drum

2) 15000 N for 2065000 cycles

   25000 N for 2600000 cycles

   30000 N for 2500000 cycles

   35000 N for 2500000 cycles

3) broken after 782000 cycles at 25000 N

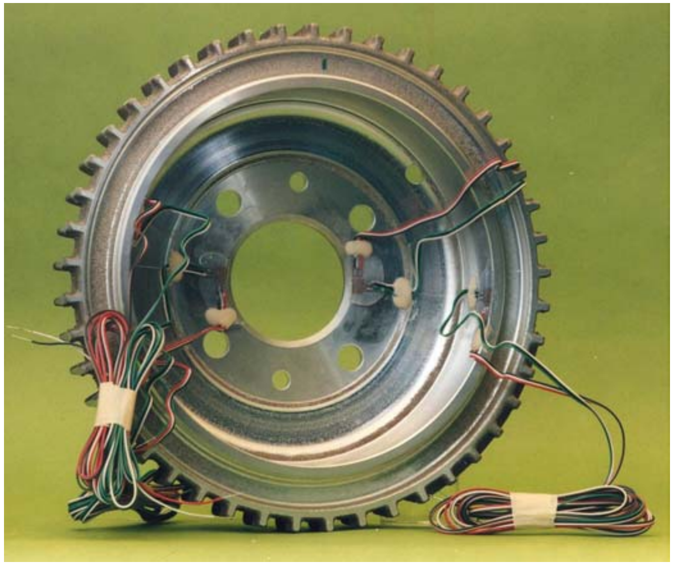

MMC Residual Stress Calculation:

$$\sigma^{i}_{tot} = \sigma_{macro} + \sigma^{i}_{mE} + \sigma^{i}_{mT}$$

i = Matrix, Reinforcement

Difference in elastic constants of the two phases

Difference in thermal expansion coefficients of the two phases

$$\sigma_{macro} = f\sigma_{tot}^{re\inf.} + (1-f)\sigma_{tot}^{matrix}$$

f **= volume fraction of the reinforcement phase**

$$\sigma^{i}_{mE} = \mathbf{B}^{i}\,\sigma_{macro}$$

B^{i} = tensor depending on reinforcement shape and elastic constants of the reinforcement and the matrix. Calculated on the basis of Eshelby's "equivalent homogeneous inclusion" model.

Before bench test

- Instrument: Neutron Diffractometer G5.2, LLB of Saclay (F)
- Wavelength: 0.316 nm
- Gauge Volume: 2x2x2 mm^3
- Diffracting plans: (200) for Al, (311) for SiC

After bench test without breaking

- Instrument: Neutron Diffractometer G5.2, LLB of Saclay (F)
- Wavelength: 0.316 nm
- Gauge Volume: 2x2x2 mm^3
- Diffracting plans: (200) for Al, (311) for SiC

After bench test with breaking

- Instrument: Neutron Diffractometer E3, HMI of Berlin (D)
- Wavelength: 0.178 nm
- Gauge Volume: 2x2x2 mm^3
- Diffracting plans: (311) for Al, (200) for SiC

Component geometry and measurement region

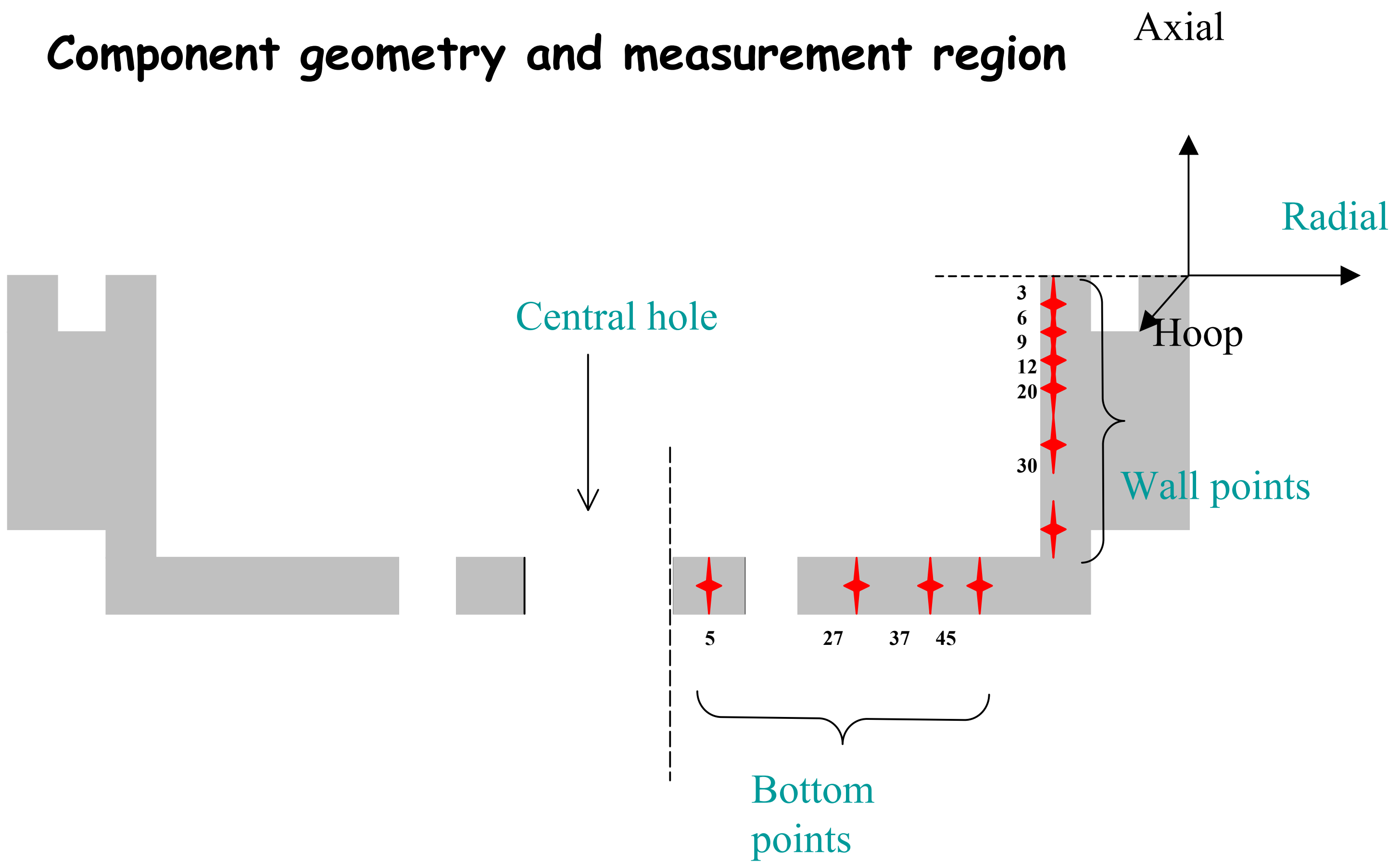

WALL

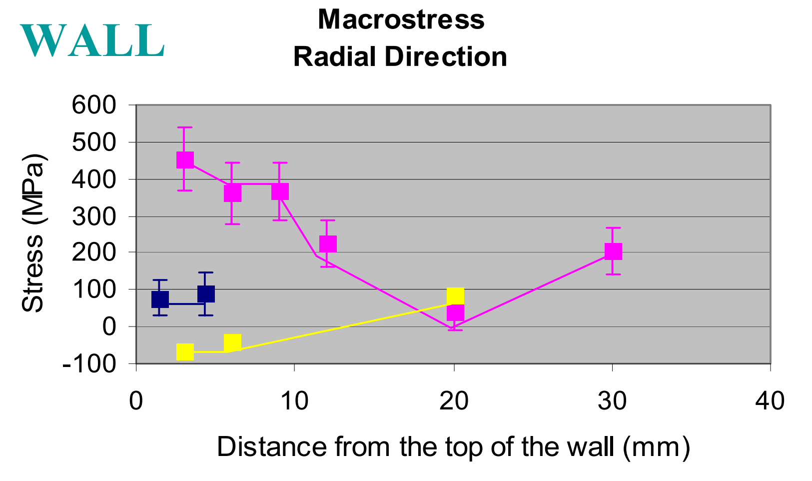

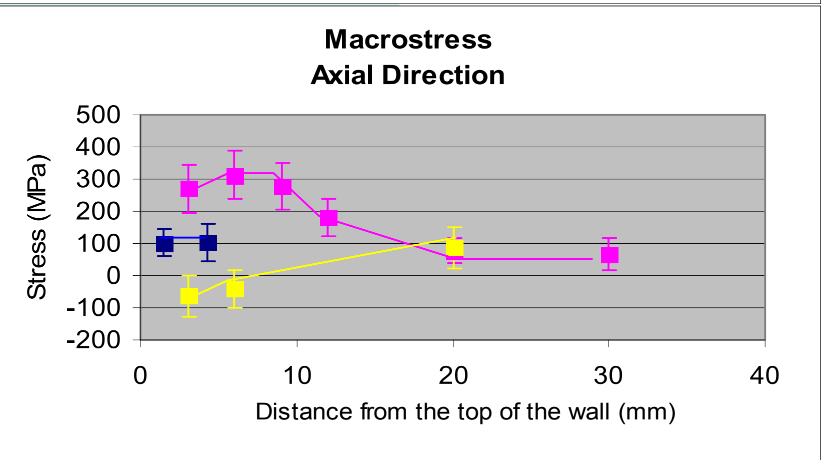

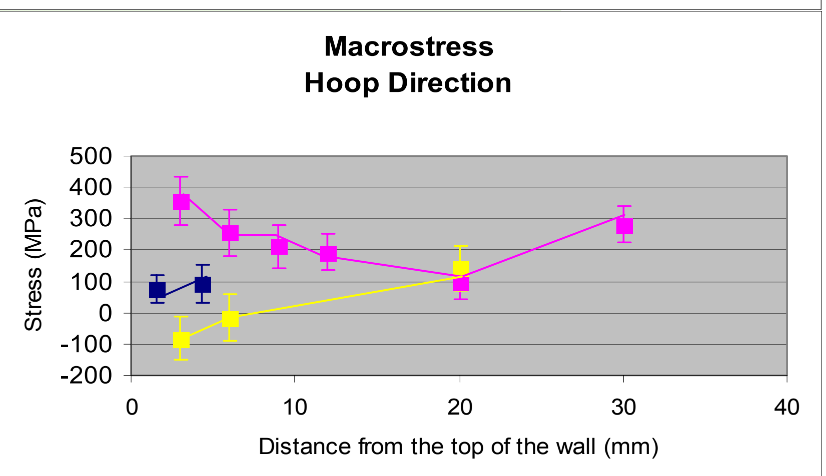

Macrostress

Residual macrostresses increase after the set of fatigue cycles without breaking.

Hoop and radial directions correspond to the highest values of stress during the in-service life of the component.

Macrostresses found before and after fatigue cycles add to the applied loads contributing to anticipate the component failure.

Macrostress

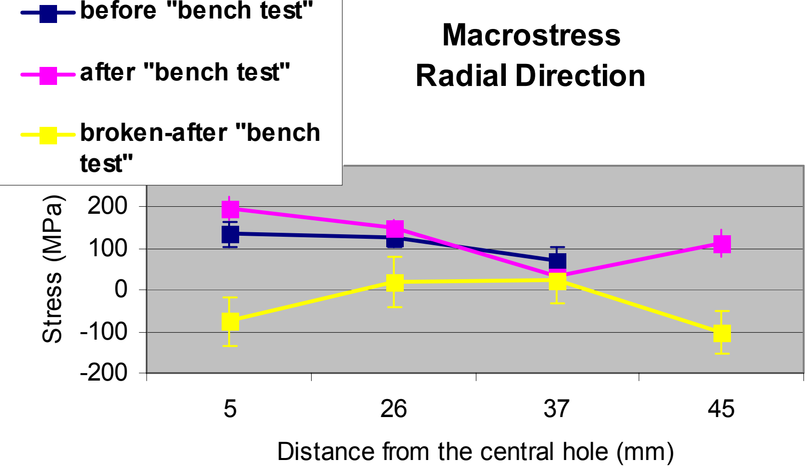

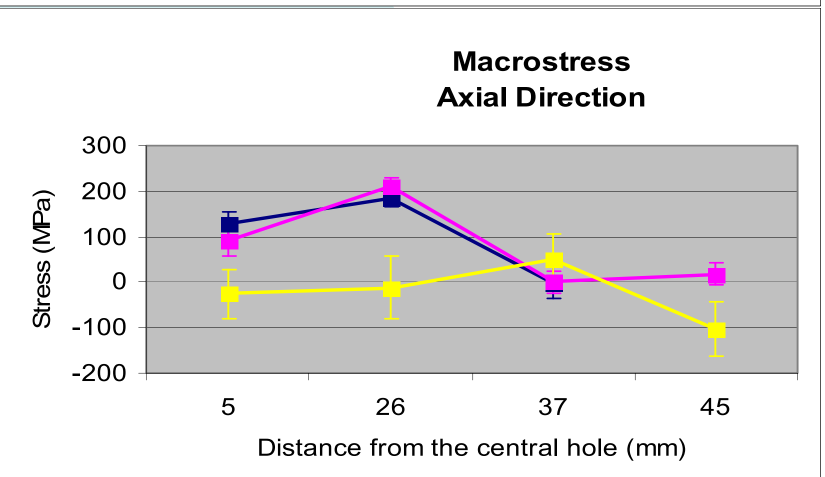

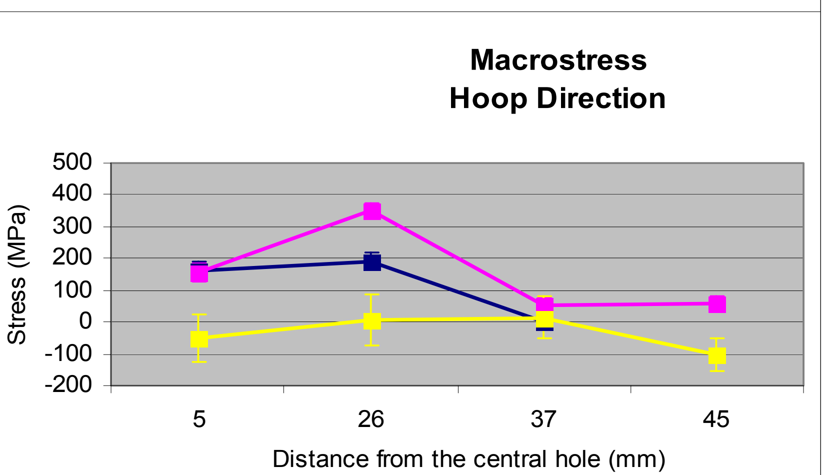

BOTTOM POINTS

Wheel Hub (AA6061 + 22 vol. % Al_2O_{3p})

3 identical wheel hubs → forging

T6: 560°C x 2 hours – H_2O at Room Temperature (RT) – 177°C x 10 hours.

T6-special: 560°C x 2 hours – H_2O at 60°C – 177°C x 8 hours.

Forging temperature	Pressure ratio	Die temperature	Oven temperature
460°C ± 20°C	Piston speed 10 mm / sec	Upper: ~ 200°C Lower: ~ 200°C	500°C x 1h 30' max

1) As-forged

2) Forged + T6 heat treatment

3) Forged + special T6 heat treatment

➢ As-forged

- Instrument: Neutron Diffractometer G5.2, LLB of Saclay (F)
- Wavelength: 0.316 nm
- Gauge Volume: 2x2x2 mm^3
- Diffracting plans: (200) for Al, (113) for Al_2O_3

Forged + T6

- Instrument: Neutron Diffractometer D1A, ILL of Grenoble (F)
- Wavelength: 0.299 nm
- Gauge Volume: 2x2x2 mm^3
- Diffracting plans: (311) for Al, (113) for Al_2O_3

➢ Forged + T6-special

- Instrument: Neutron Diffractometer D1A, ILL of Grenoble (F)
- Wavelength: 0.299 nm
- Gauge Volume: 2x2x2 mm^3
- Diffracting plans: (311) for Al, (113) for Al_2O_3

Wheel hub - Measurement points

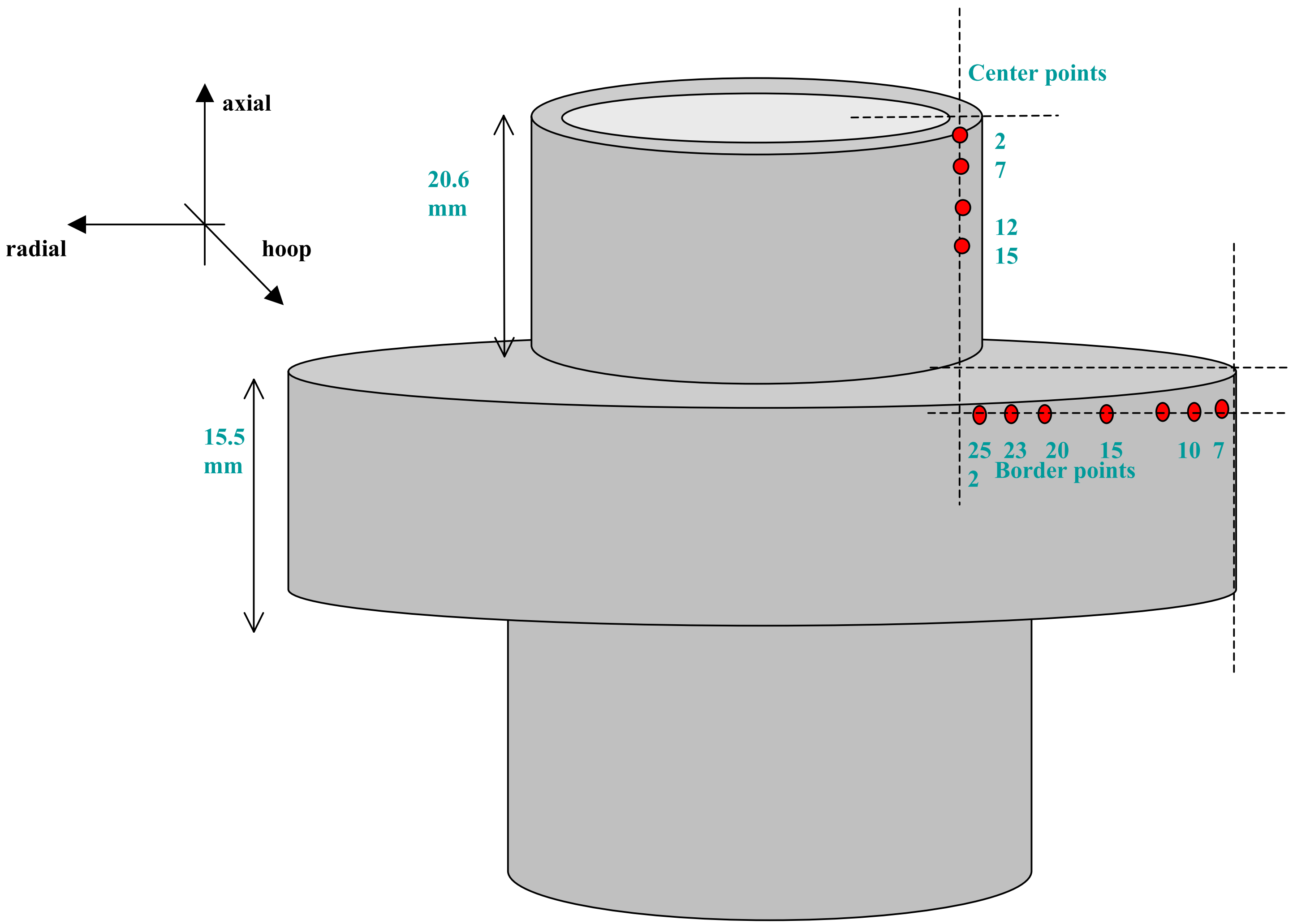

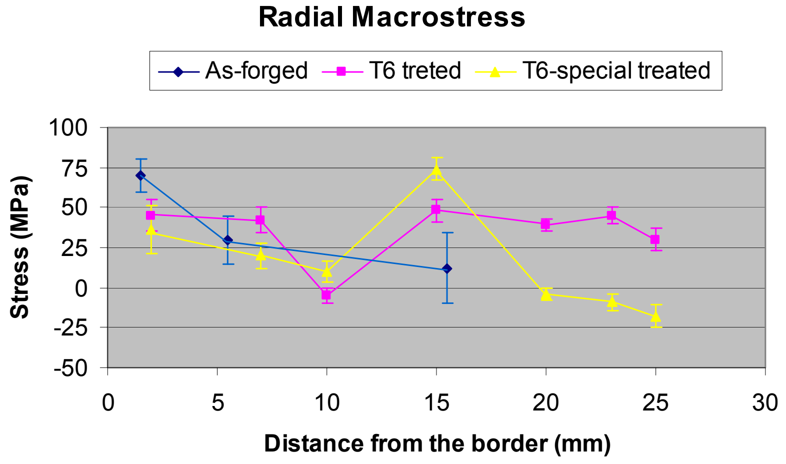

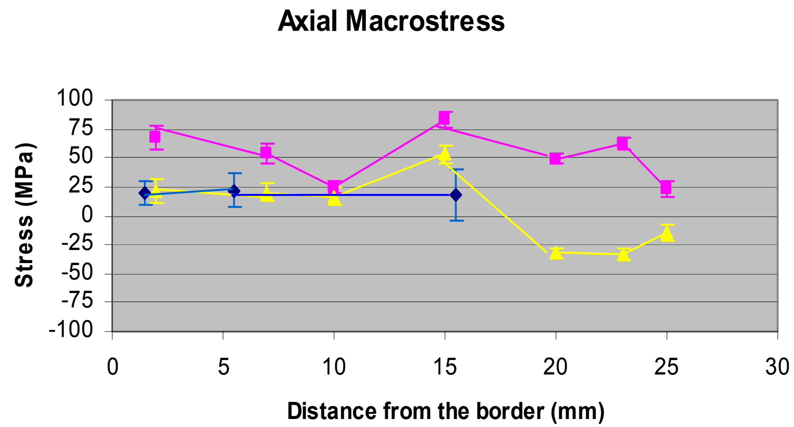

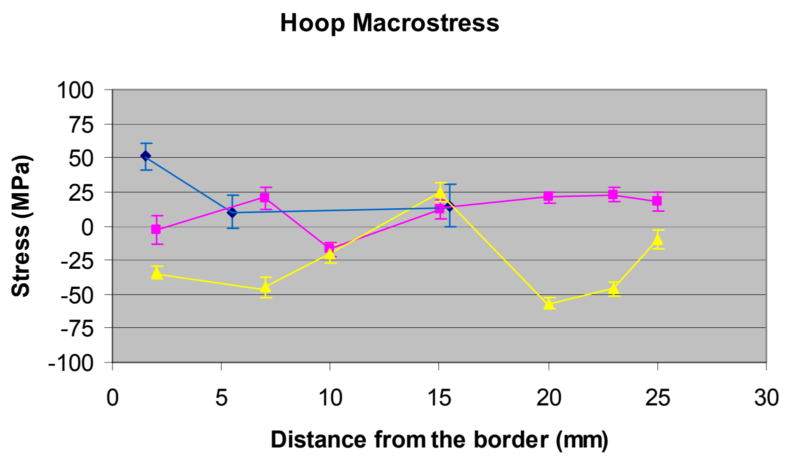

Macrostress

- **Before heat treatments, the macrostresses are mainly located close to the border (in radial and hoop directions).**
- **Radial and hoop macrostress at the surface are reduced by T6 heat treatment.**
- **In the case of the T6-special treated hub , the macrostresses are lower than in the previous case (T6 treatment).**

T6 and T6-special treatments improve mechanical performances, because they reduced residual macrostress close to the surface, in the directions (hoop and radial) critical during service.

$$\sigma^{i}_{tot} = \sigma_{macro} + \sigma^{i}_{mE} + \sigma^{i}_{mT}$$

i = Matrix, Reinforcement

Difference in elastic costants of the two phases

Negligible

Difference in thermal expansion coefficients of the two phases

microstress monitoring

after mechanical and/or thermal treatments

Thermal mismatch Microstress

WHEEL HUB (BORDER POINTS)

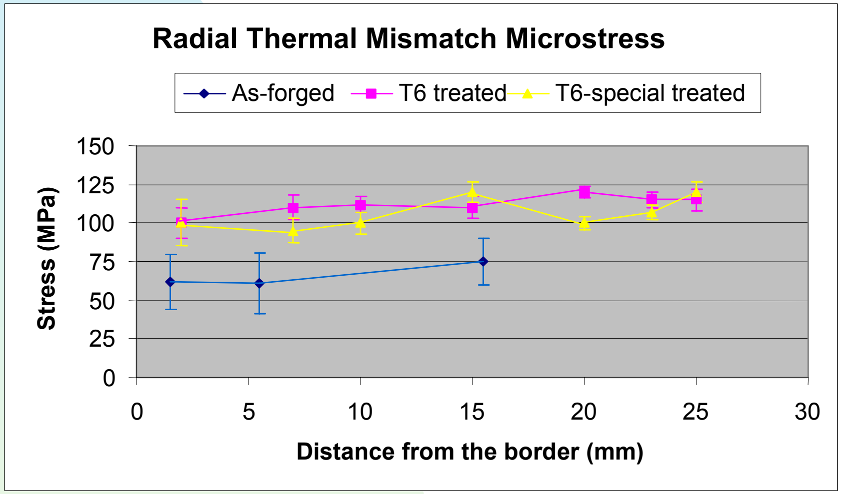

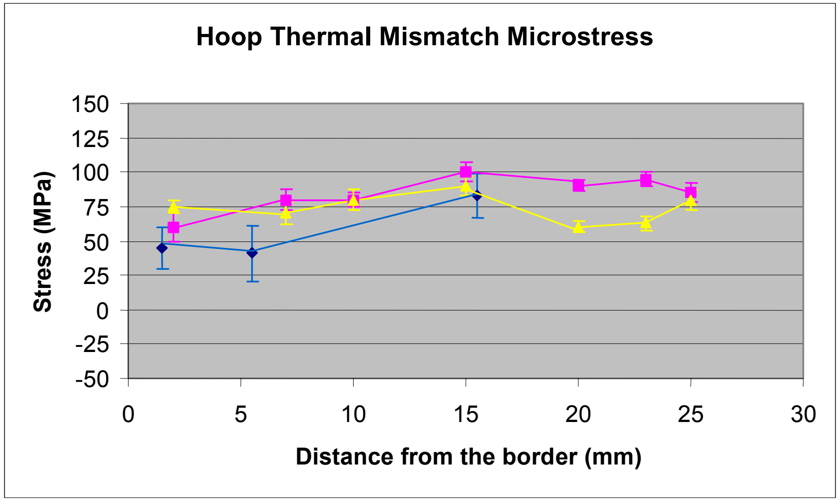

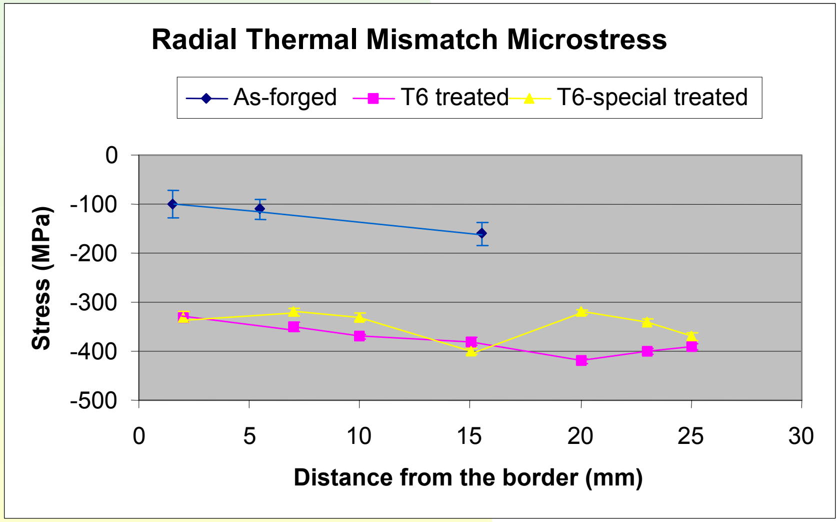

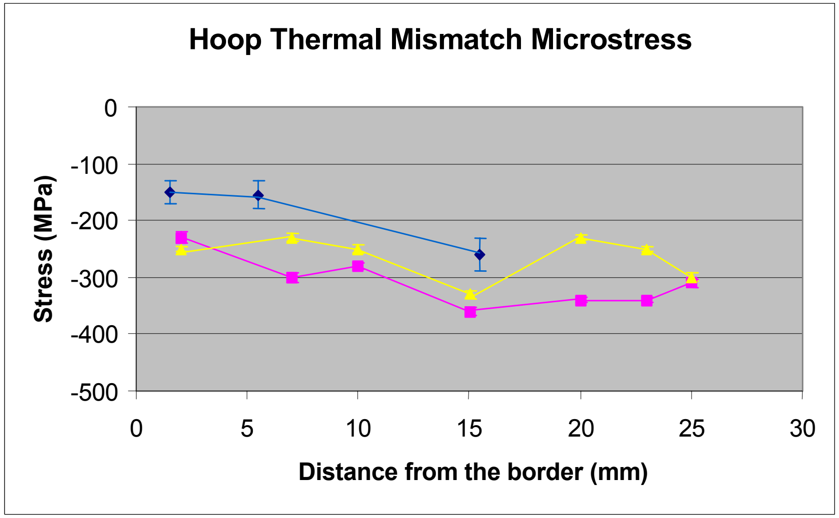

Thermal mismatch microstresses increase (in absolute value) after T6 and T6-special heat treatments.

Reduced effect in the T6-special treated hub

T6-special treatment:

Good compromise to reduce macrostress
without having too high thermal mismatch microstresses values.

Fatigue cycles induce a thermal microstress releasing

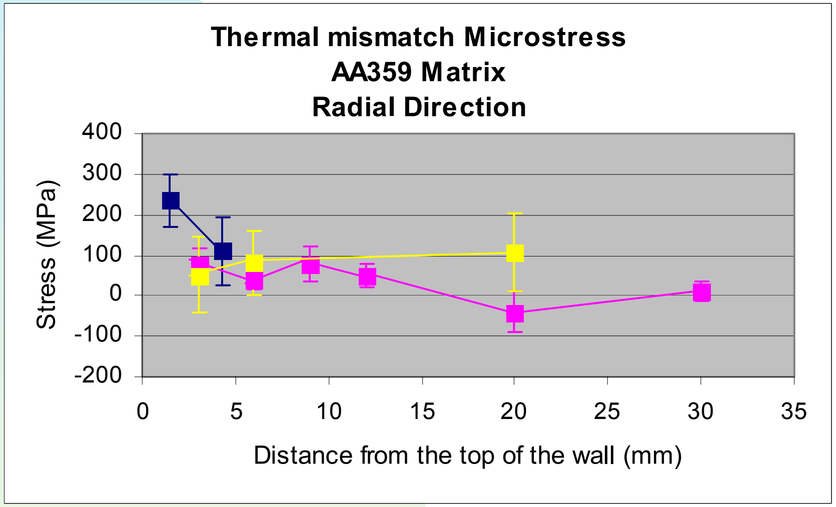

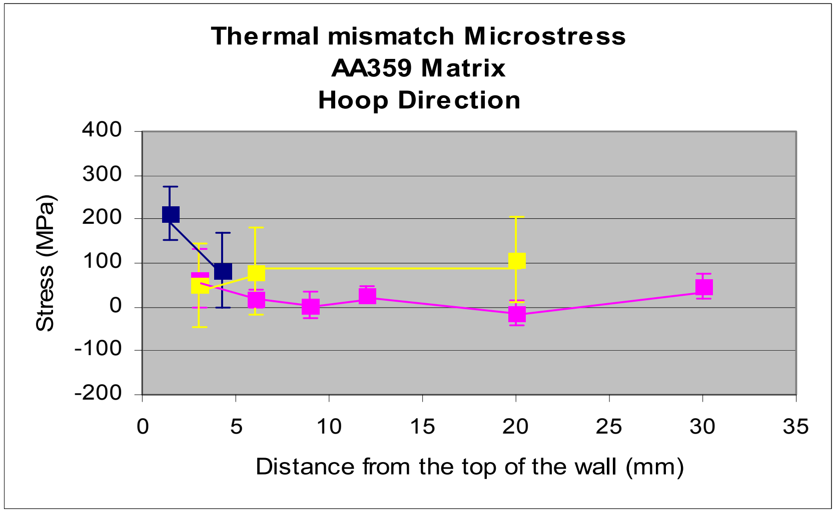

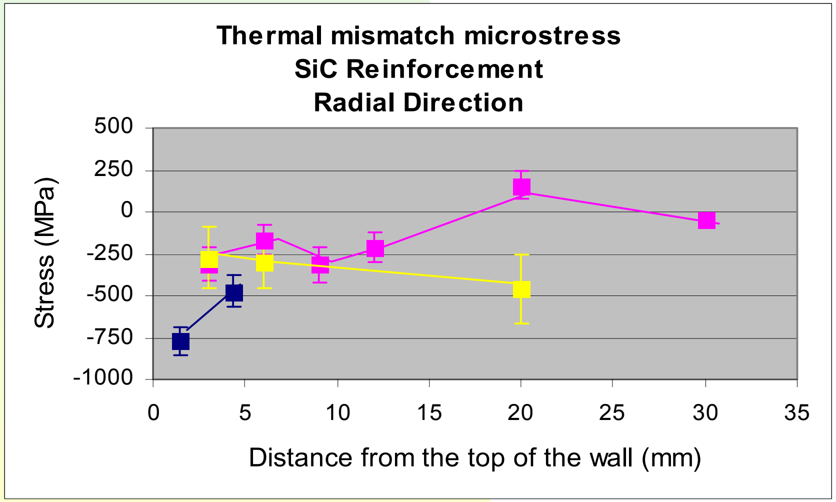

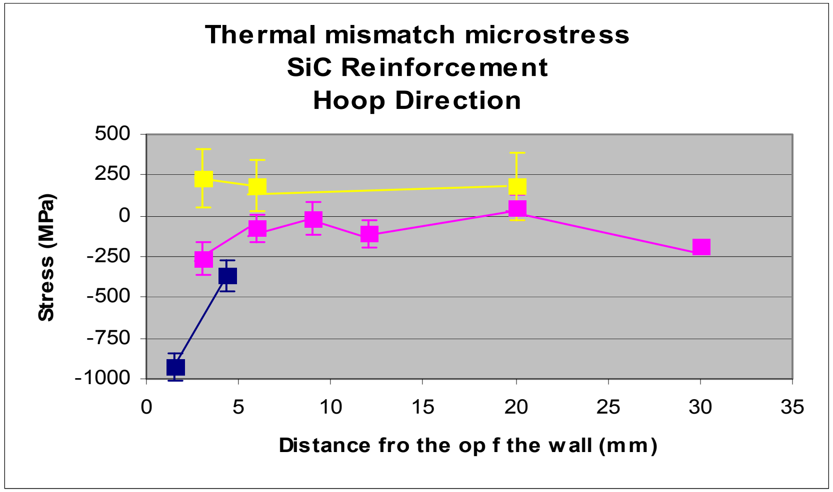

Conclusions

AA359+SiC Brake Drum

AA6061+Al2O3 Wheel Hub

RESIDUAL MACROSTRESS

⇧ AFTER FATIGUE CYCLES

⬇ AFTER T6 AND T6-SPECIAL TREATMENTS (SURFACE)

THERMAL MISMATCH MICROSTRESS

RELEASE AFTER FATIGUE CYCLES IN BOTH THE PHASES

INCREASE AFTER T6 AND T6-SPECIAL TREATMENTS IN BOTH THE PHASES

Simulation of the forming process and comparison between calculated and experimental results

The present study is part of the European project COFCOM (contract N° BRPT-CT97-803).

HMI-BENSC is acknowledge for beamtime allocation and financial support in the frame of the EU programme “Access to Large Scale Facilities”.

Component: Drive Shaft for Helicopter

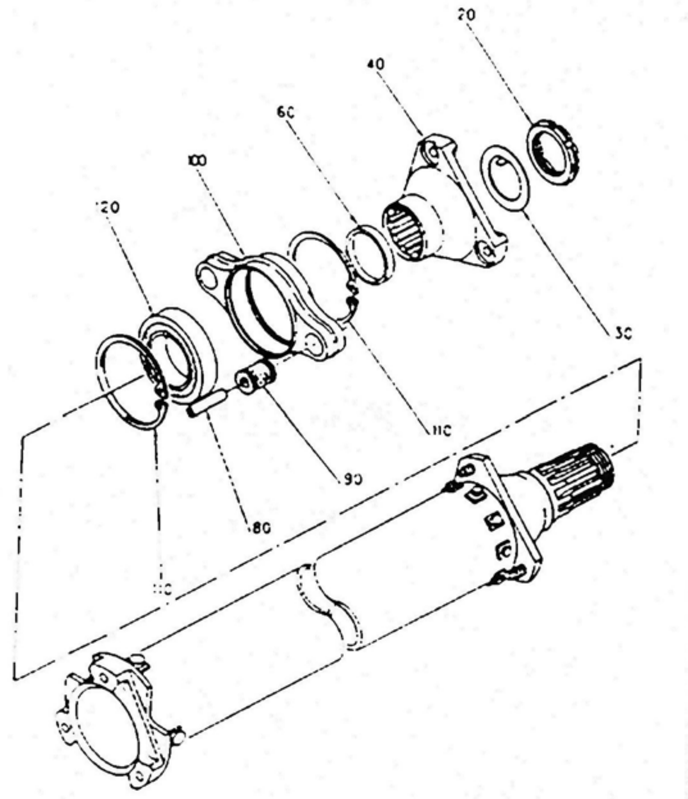

Material:
MMC AA2009 + 25% SiCp

Matrix composition:

	Cu	Mg	Si	O	Fe	Zn	other	Al
Min	3,2	1	-	-	-	-	-	remaining
Max	4,4	1,6	0,25	0,60	0,20	0,10	0,15	

Reinforcement:
SiCp particles

H and Cubic structure

The complete study has been carried out in several steps:

1/ Characterisation of the billet as fabricated (Powder Metallurgy)

2/ Characterisation of the test specimens after tensile tests

3/ Results used as input for the model to simulate the extrusion process

4/ Extrusion of a thick tube with the conditions simulated

3/ Characterisation of the demonstrator (thick tube Ø80mm thickness 19 mm as extruded and after T4 thermal treatment (498° C for 4h, followed by water quenching and natural ageing)

We will present only the University of Ancona’s work on the residual stress analysis (points 1 and 5) and compare these results with the numerical simulation performed by the Univeristy of Galway (Ireland) (point 3).

The characterisation of the tensile speciment has been performed by the University of Catalunya (Barcelona, Spain), and the extrusion by British Aluminium (Redditch, Great Britain)

Extrusion process: indirect extrusion

Parameters:

θ container: 430°C

θ billet: 465°C

Speed: 0,5m/mn

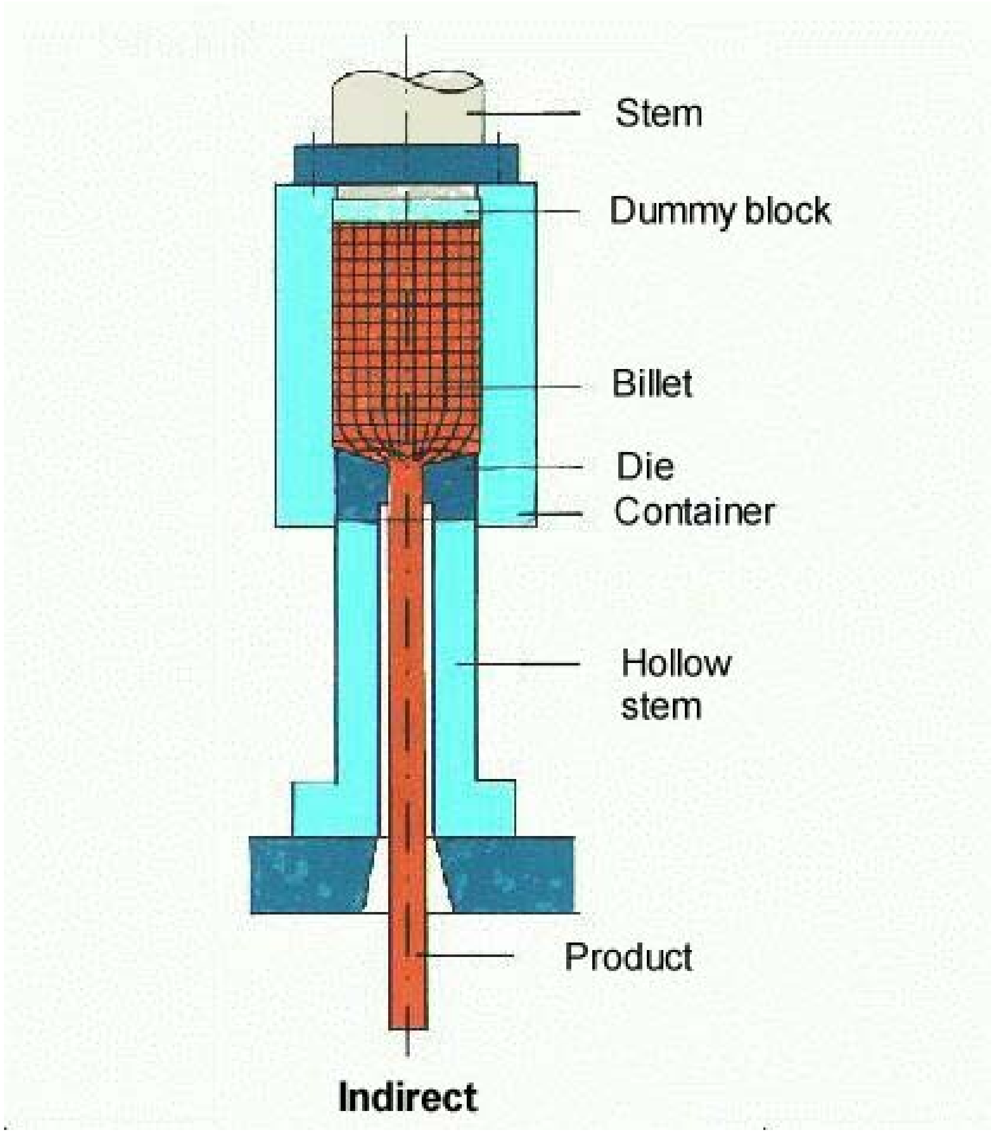

Results

All the measurements have been performed at the neutron diffractometer E3 of the HMI (Berlin, Germany).

λ= 1,37 Å

Gauge volume size: 3x3x2 mm^3

Investigated Bragg Peaks: Al(420) $\rightarrow 2\theta = 68°$

SiC(311) $\rightarrow 2\theta = 62°$

Elastic constants taken from the litterature*:

Al: E=69 GPa ν=0,35

SiC: E=384 GPa ν=0,20

*B.Eigenmann, E.Macherauch, Matt.-wiss. u. Wrkstofftech. 27, 426-437 (1996)

•Billet prepared by standard powder metallurgical route (as fabricated) with dimensions 356 mm diameter, 30 mm height.

Very low residual stresses: around 10 MPa in the aluminium and -50 MPa in the SiC.

Simulation of the extrusion process

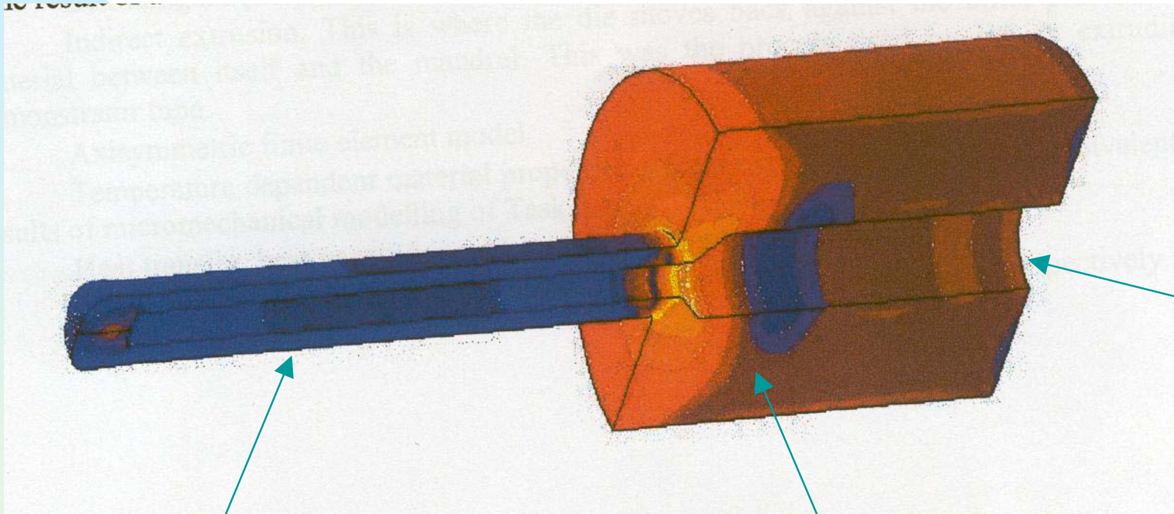

Direction of extrusion

Extruded tube

Results of the simulation

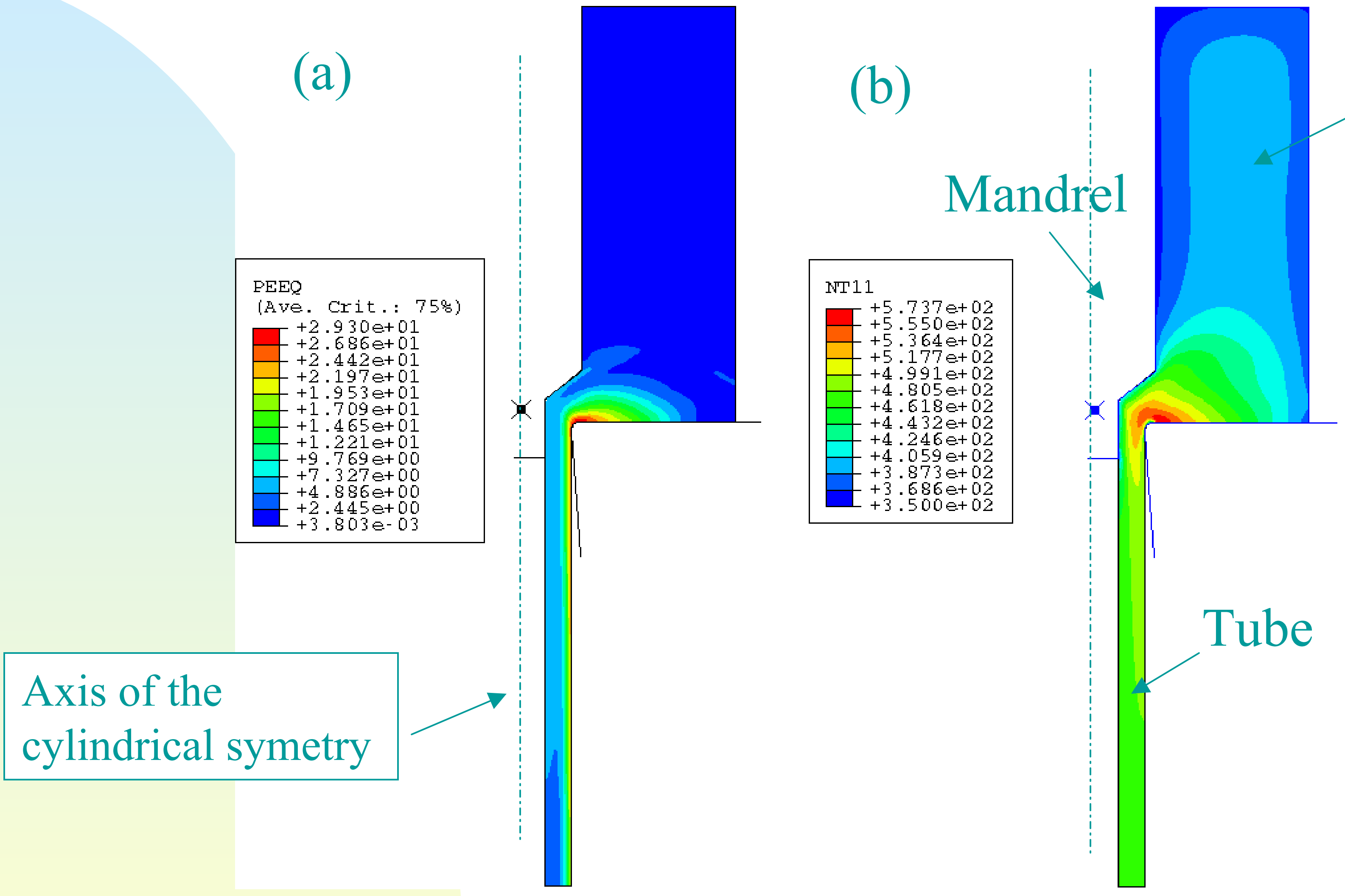

Distribution of (a) equivalent plastic strain and (b) temperature (°C).

The temperature distribution and the equivalent plastic strain at the end of the extrusion process are essentially constant in depth and along the cylinder axis.

The temperature gradient through the extruded tube is insignificant $\Rightarrow$ the residual stress in the tube will not be affected by uniform cooling.

Experimental results

Macro Stress (MPa)		Average error ±40 MPa	
Sample	Axial	Radial	Hoop
As extruded	74	69	71
T4	80	27	43

Table 1: Ma

T4 thermal treatment

⇓

the *macro-stress* relaxes in the radial and hoop directions and remains constant in the axial one

	Al	Average error:	± 35 MPa	SiC	Average error:	± 35 MPa
Sample	σ_{ax}	σ_{rad}	σ_{hoop}	σ_{ax}	σ_{rad}	σ_{hoop}
As extruded	135	109	120	-109	-49	-73
T4	163	98	126	-171	-183	-206

Table 2: Total stress in the principal directions for the two tubes

T4 thermal treatment

⇓

Nevertheless, *total stresses* remain almost constant in the Al matrix and increase in the SiC reinforcement

	Al	Average error:	± 35 MPa	SiC	Average error:	± 35 MPa
Sample	σ_{ax}	σ_{rad}	σ_{hoop}	σ_{ax}	σ_{rad}	σ_{hoop}
As extruded	83	40	49	-183	-118	-144
T4	83	71	83	-251	-210	-249

Table 3: Microstress in the principal directions for the two tubes

T4 thermal treatment

$\Downarrow$

This implies that both the tensile *micro-stresses* in the Al phase and the compressive *micro-stresses* in the SiC phase increase (of about 30 MPa for the Al phase and 70 to 100 MPa for the SiC phase).

Although error bars are relatively large, this behaviour is to be expected and exceeds the confidence limits.

Conclusion

As expected, results show that the main contribution to residual stress is generally given by **thermal microstresses**.

If the macrostress is vanishing (in the billet) ⇒ thermal mismatch stresses stay very small

In the tube: macrostresses are constant along the thickness and decrease on application of the thermal treatment, while microstresses increase.

This effect can be observed only using Neutron Diffraction as evaluation technique.

Numerical simulations are in good agreement with experiments and preedict very low macrostress in the extruded tube.

Stress field around cracks in AA2024

Collaboration with University of Naples and Alenia Aeronautica S.p.A.

- General aim:

Investigation of crack nucleation and propagation (phenomenology, including first stages short cracks), also in the light of most recent theories (K.Sadananda, A.K.Vasudevan, *Int. J. Fatigue*, Vol.19, N.1 (1997) S99)

- Studied materials: Al alloys for aircraft structural parts (cracks in the neighborhood of rivets)

- FEM models experimental validation (neutron and synchrotron radiation measurements)

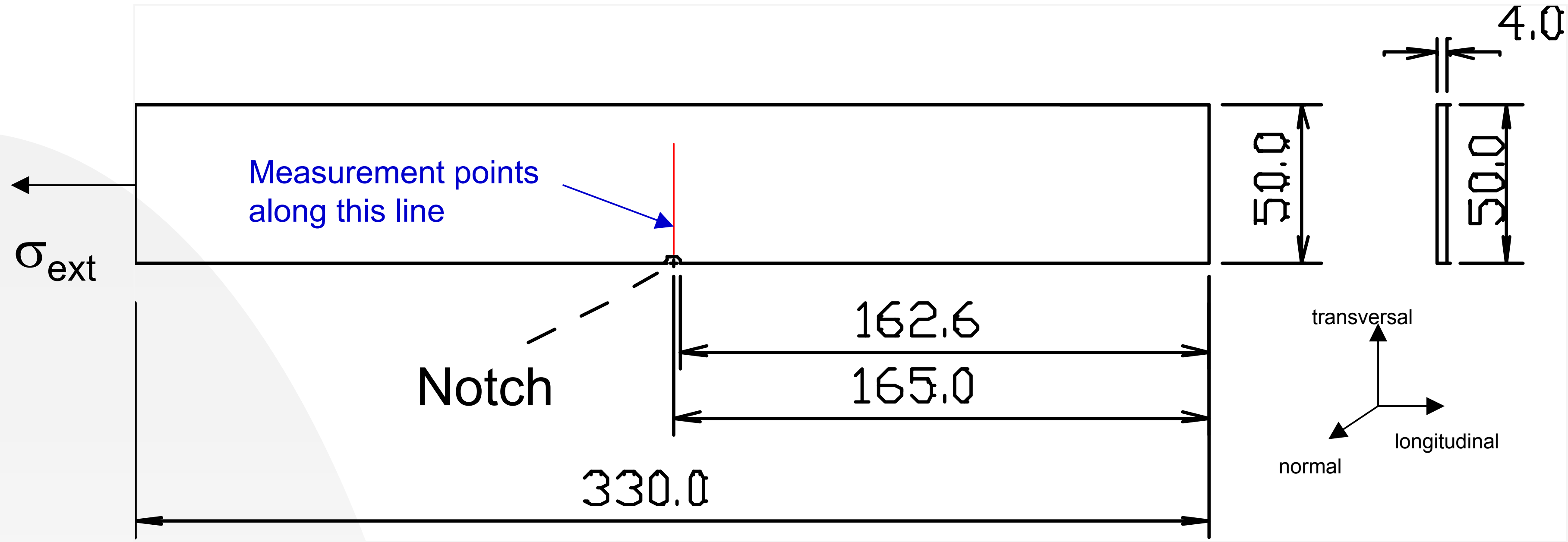

- precycled: $R = 0.06$, $\sigma_{max} = 90$ MPa;
- crack length: about 4 mm from the notch (transversal direction);
- plane stress assumed ($\sigma_{normal} = 0$), due to specimen geometry.

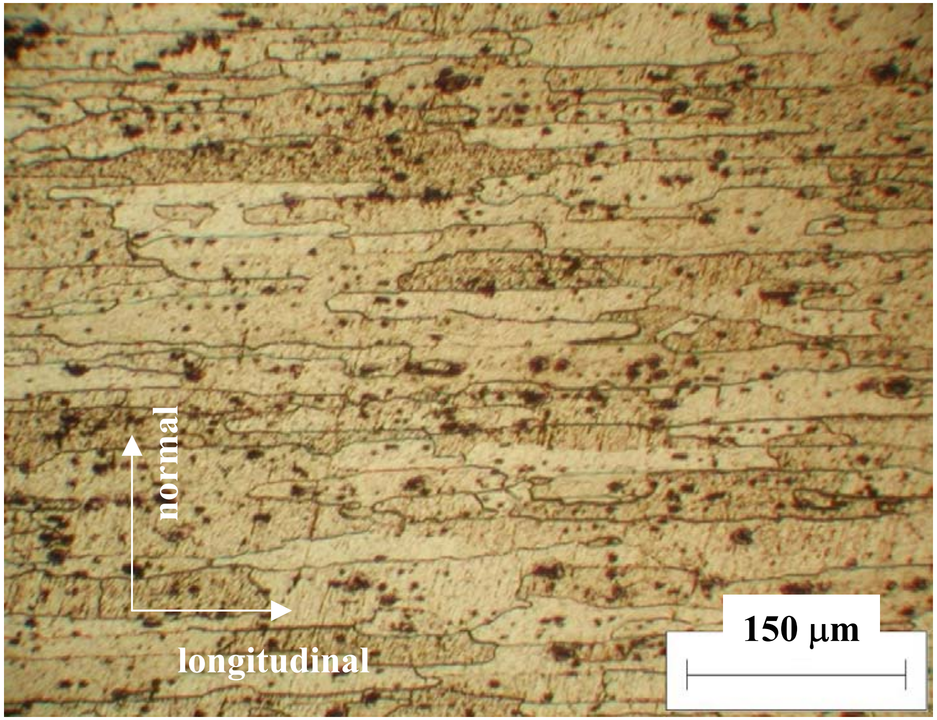

Measurements at LLB-Saclay

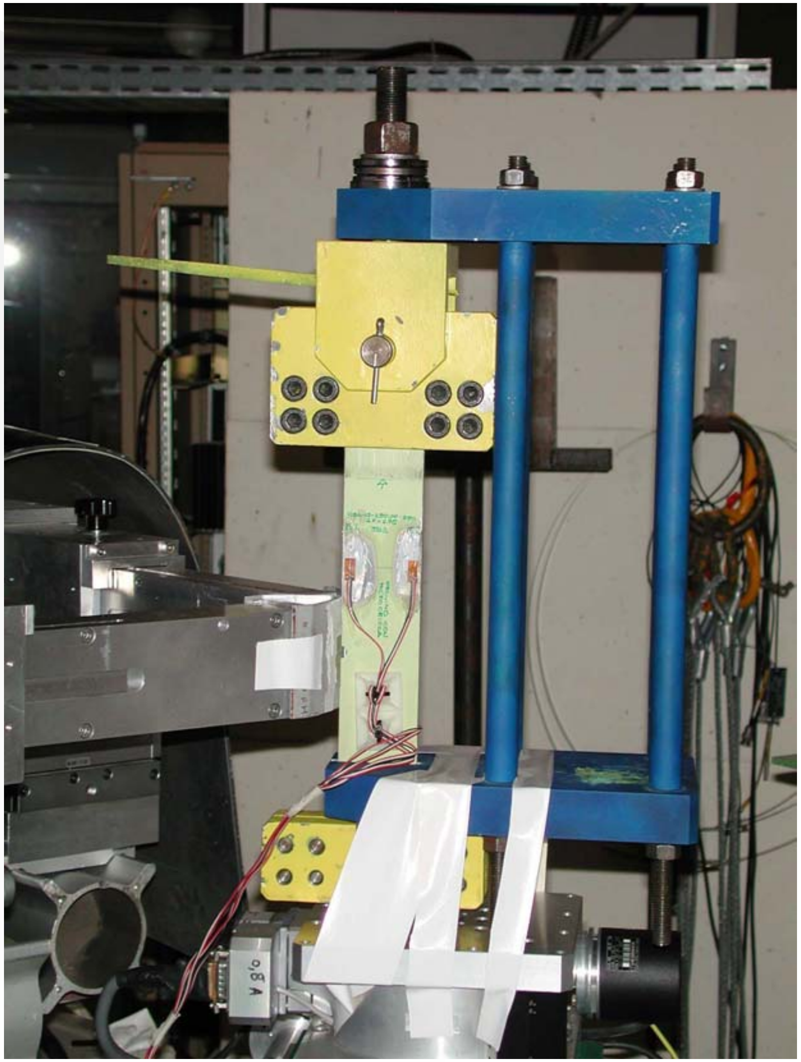

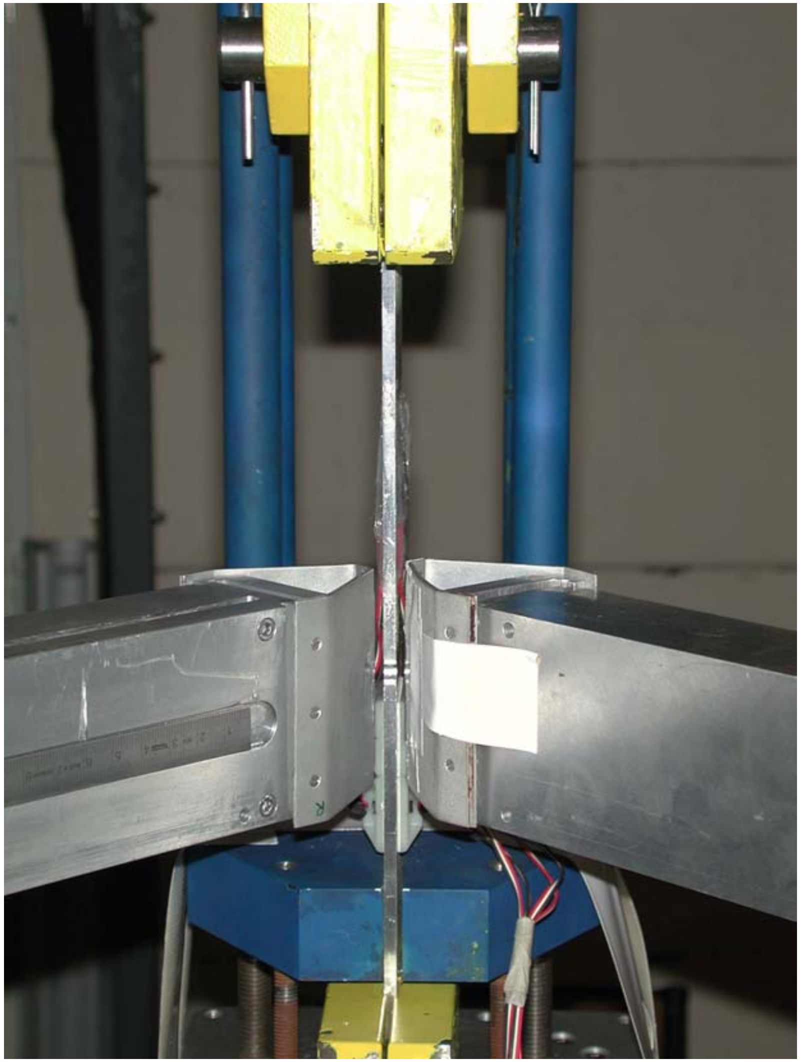

Experimental conditions

- σ_{ext} = 45 MPa
- λ = 0.33 nm, (111) Al Bragg peak
- gauge volume: 0.8 x 0.5 x 1 mm^3
- longitudinal and transversal strain directions investigated
- d_0 measured in a point far from the crack

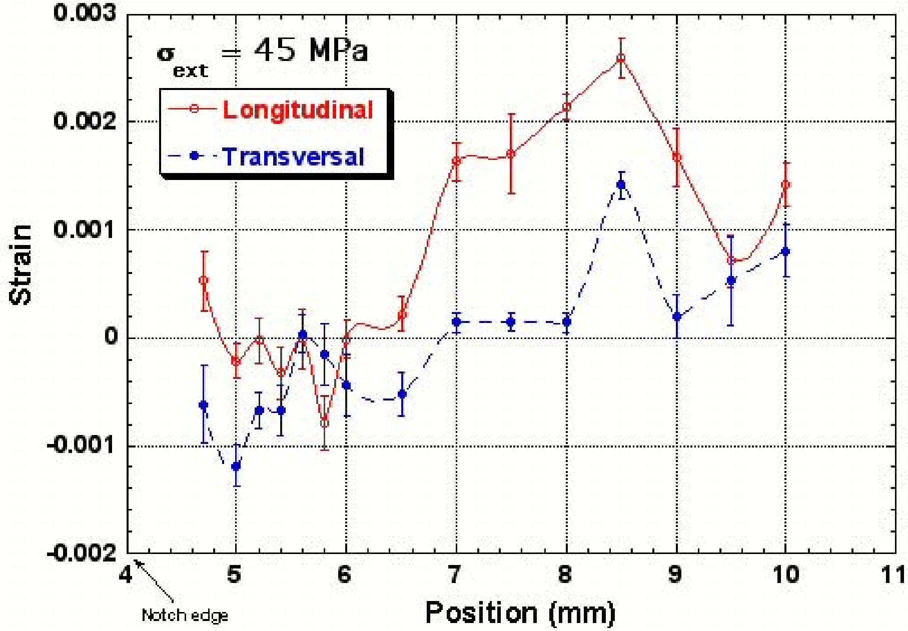

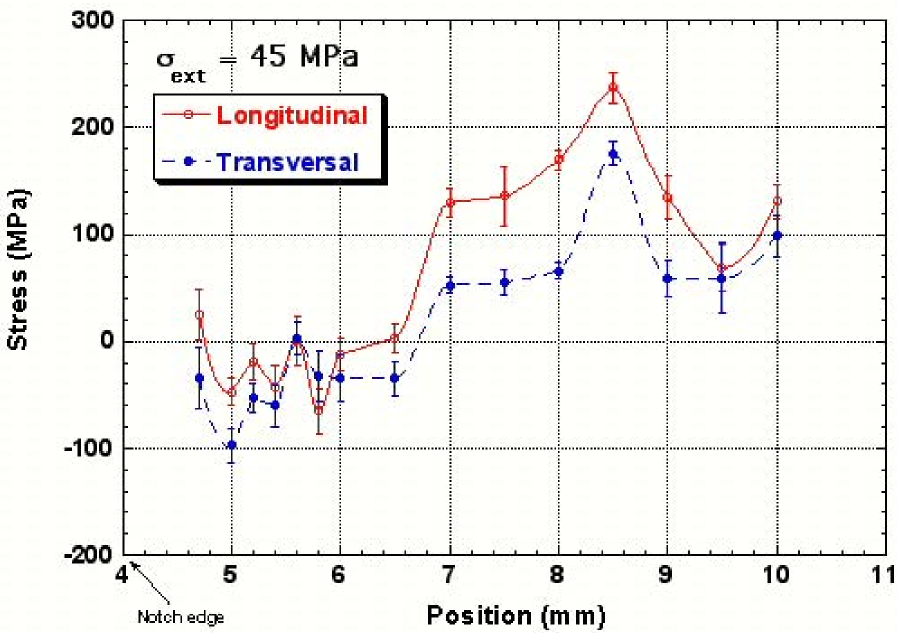

$$\sigma_L = \frac{E}{1-\nu^2}\left(\varepsilon_L + \nu\varepsilon_T\right)$$

$$\sigma_T = \frac{E}{1-\nu^2}\left(\varepsilon_T + \nu\varepsilon_L\right)$$

$$\sigma_N = 0$$

• Results will be compared with FEM calculations (carried out by University of Naples)

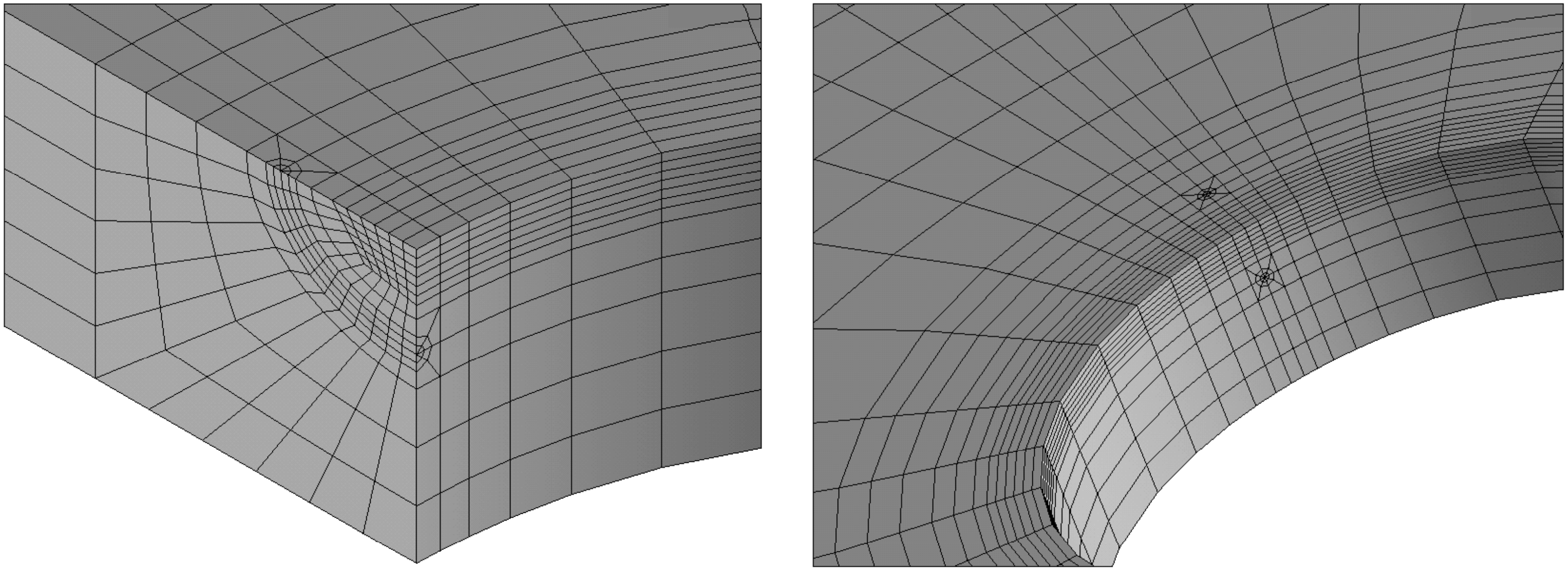

• Short crack (0.2 mm) recently investigated by synchrotron radiation (6-10 Nov. @ ESRF - data analysis in progress)

AA6082 Shrink-Fit Systems

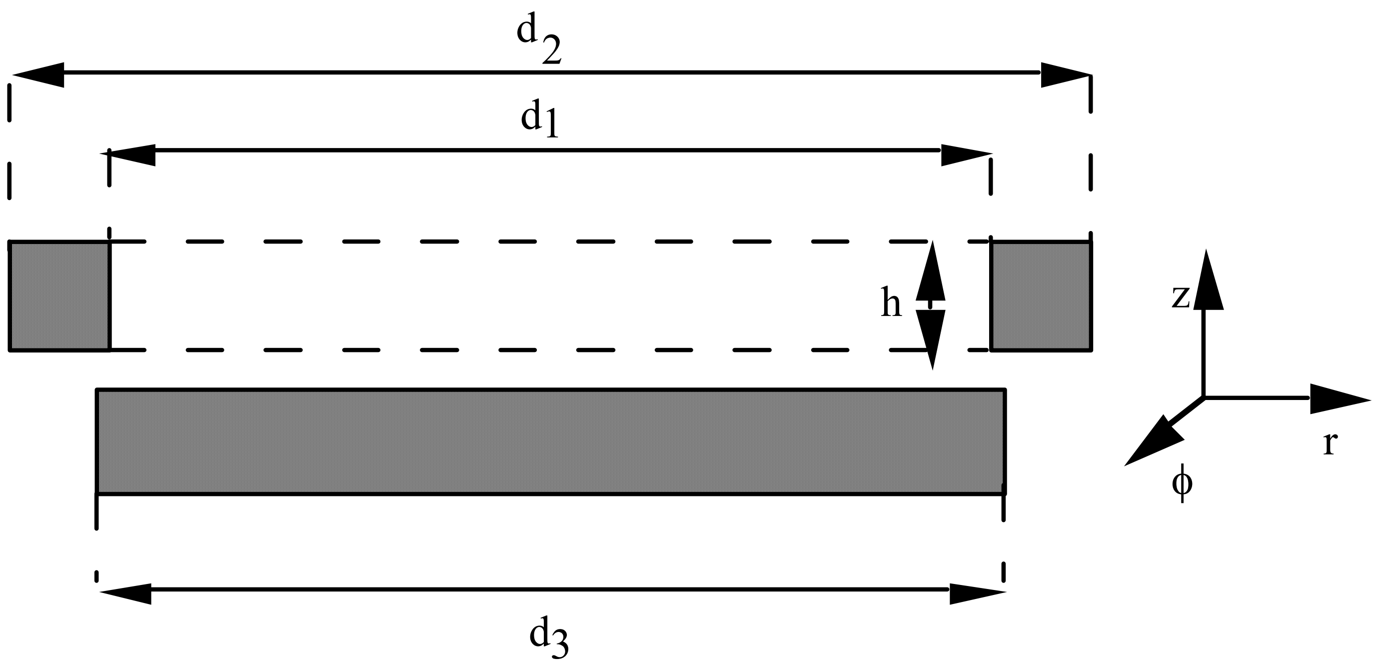

d_1 = 100 mm

d_2 = 119 mm

d_3 = 100.230 mm

h = 15 mm

$i = d_3 - d_1$ = 230 µm

FEM RESULTS

Thermoelastic

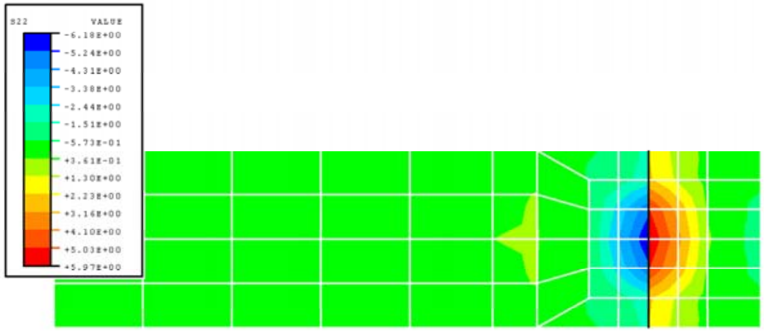

(a)

(b)

(c)

Thermoelastoplastic

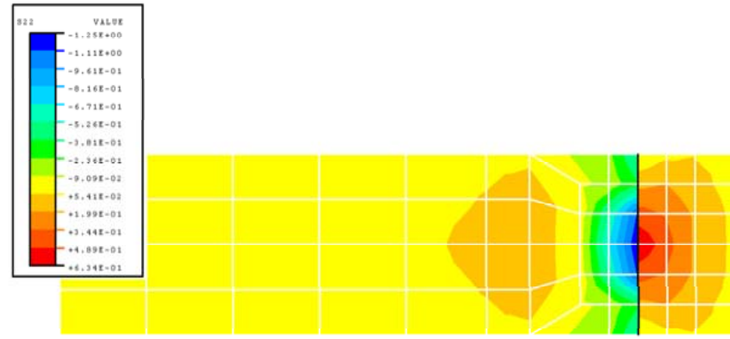

(a)

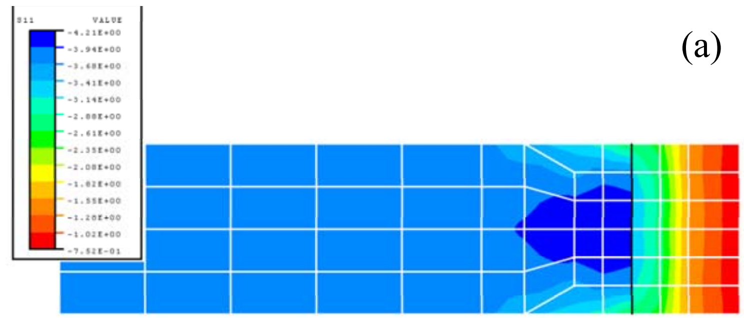

(b)

(c)

a) axial; b) radial; c) hoop

NEUTRON DIFFRACTION

- G5.2 diffractometer of LLB, Saclay (F)
- (200) Bragg peak was used (d_{200}≈2.024 Å)
- neutron wavelength λ=2.84 Å
- 13 gauge points were investigated (6 in the disc, 7 in the ring)
- gauge volume = 1.1 mm (basis diameter) x 3 mm (height) cylinder

Unstrained interplanar distance d_0 (imposing biaxial stress):

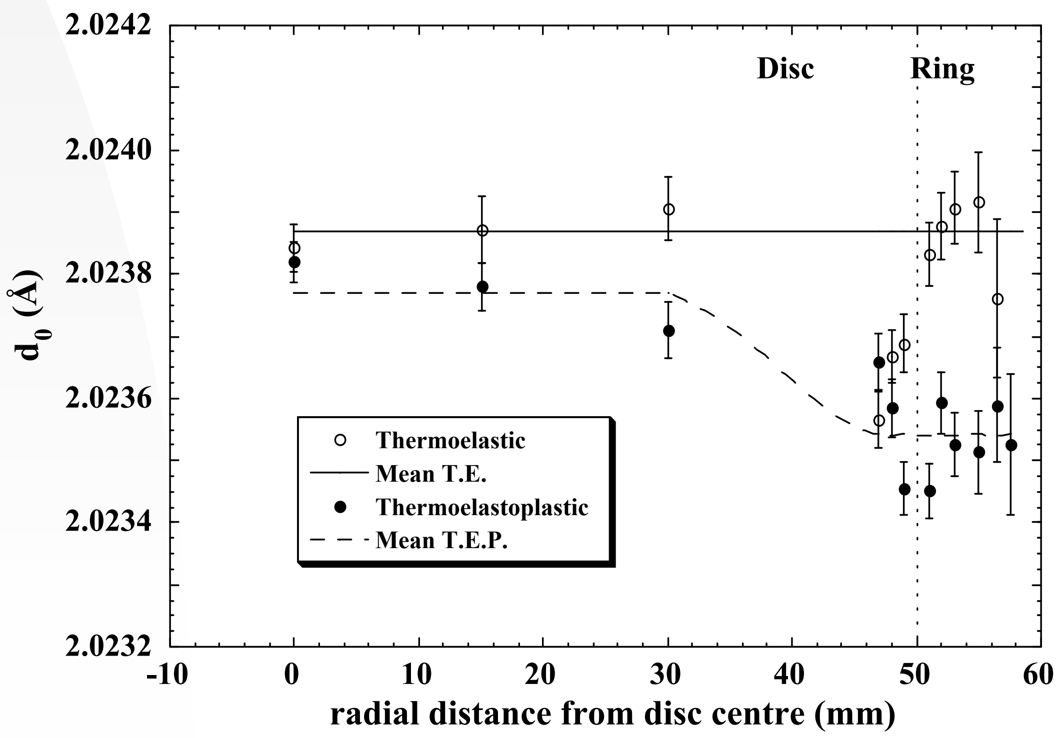

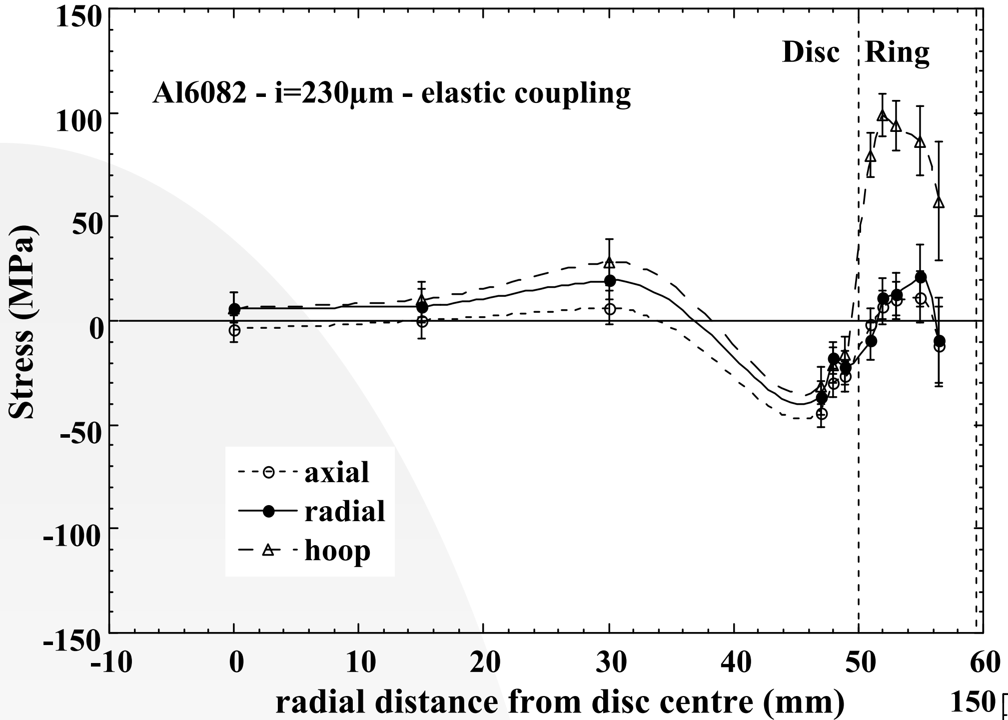

Good agreement with FEM calculations

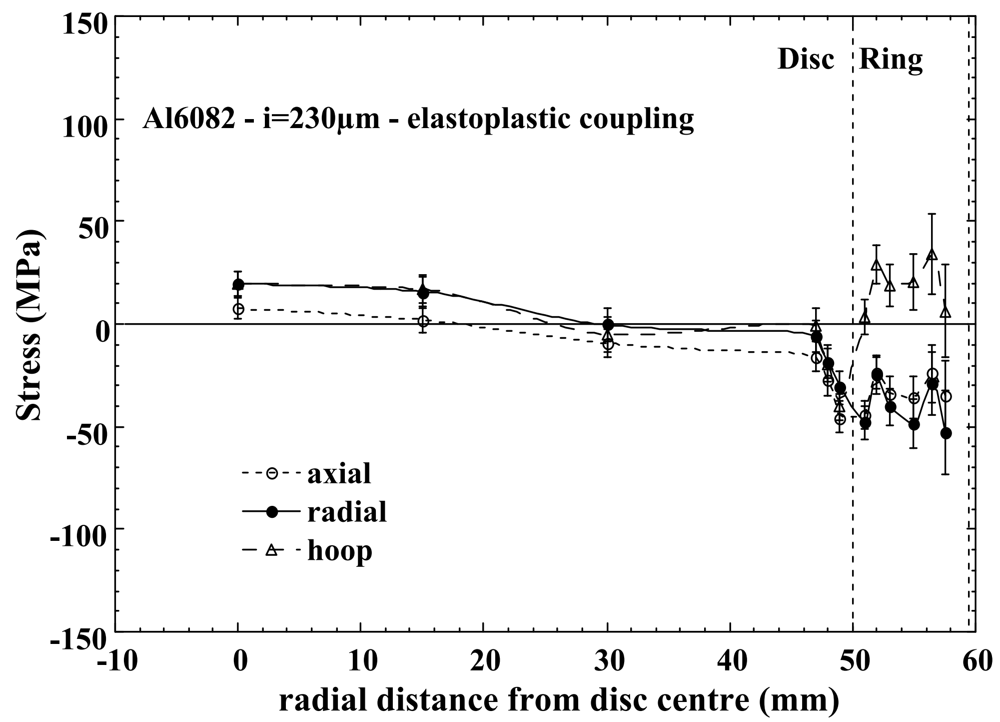

AA6082 Shrink-Fit Systems

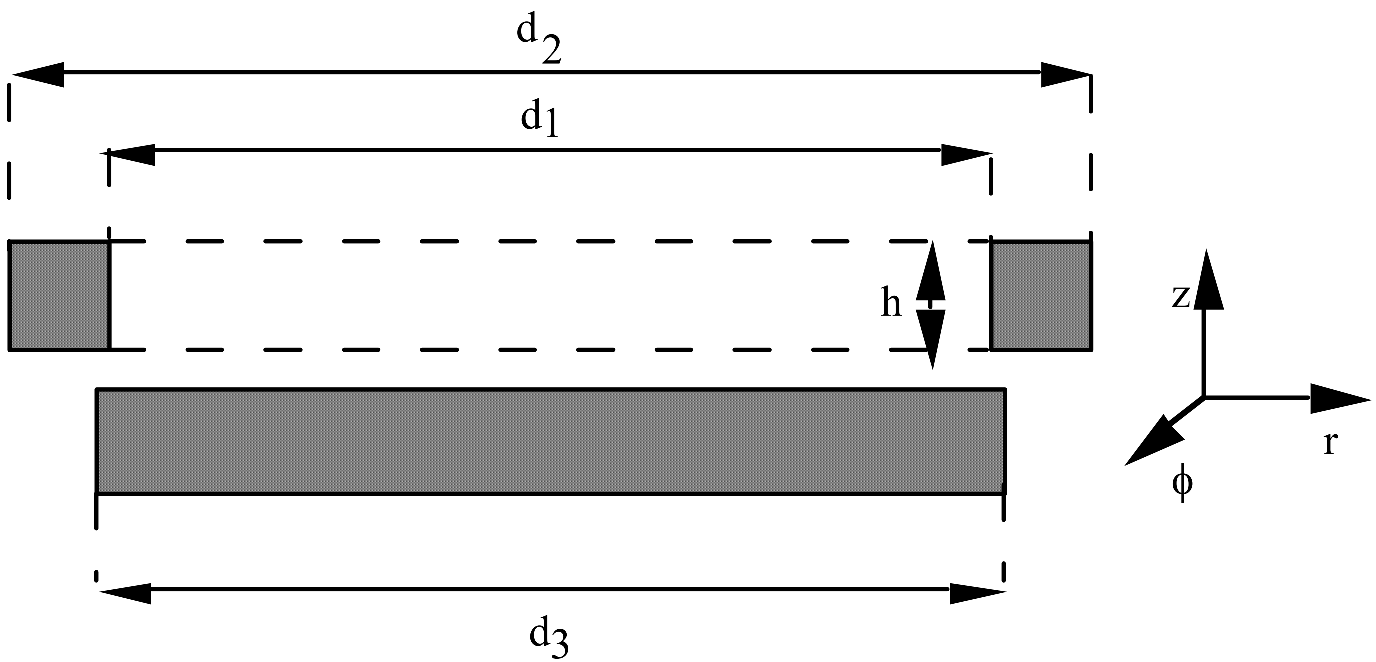

$d_1 = 100$ mm

$d_2 = 119$ mm

$d_3 = 100.230$ mm

$h = 15$ mm

$i = d_3 - d_1 = 230\ \mu m$

FEM RESULTS

Thermoelastic

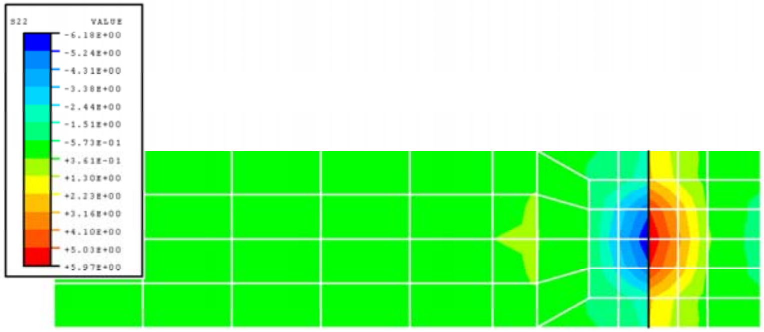

(a)

(b)

(c)

Thermoelastoplastic

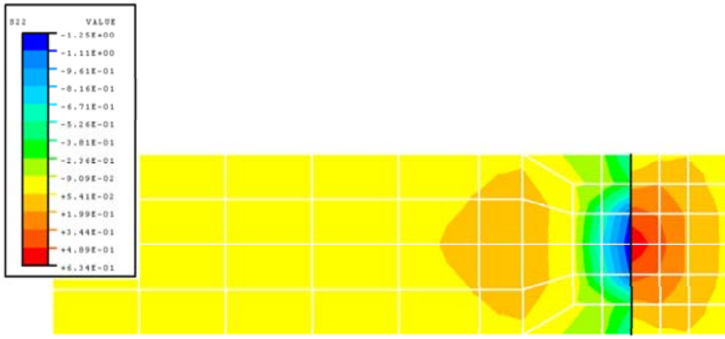

(a)

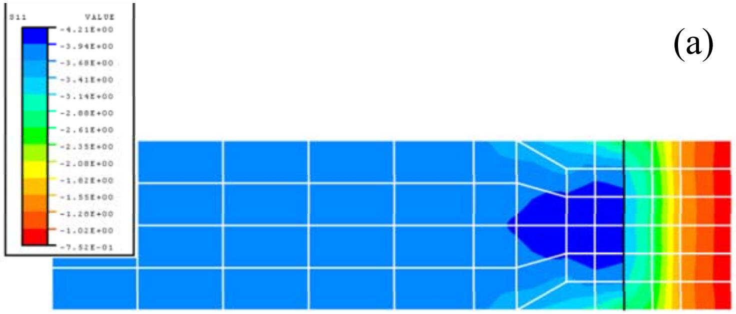

(b)

(c)

a) axial; b) radial; c) hoop

NEUTRON DIFFRACTION

- G5.2 diffractometer of LLB, Saclay (F)
- (200) Bragg peak was used (d_{200}≈2.024 Å)
- neutron wavelength λ=2.84 Å
- 13 gauge points were investigated (6 in the disc, 7 in the ring)
- gauge volume = 1.1 mm (basis diameter) x 3 mm (height) cylinder

Unstrained interplanar distance d_0 (imposing biaxial stress):

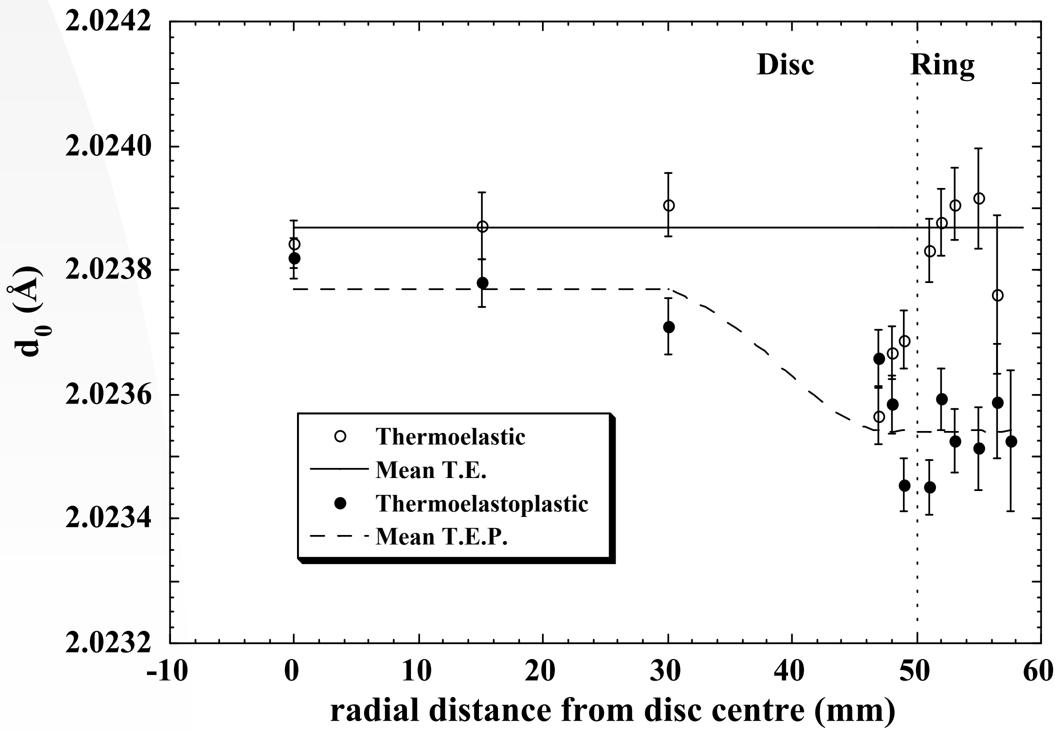

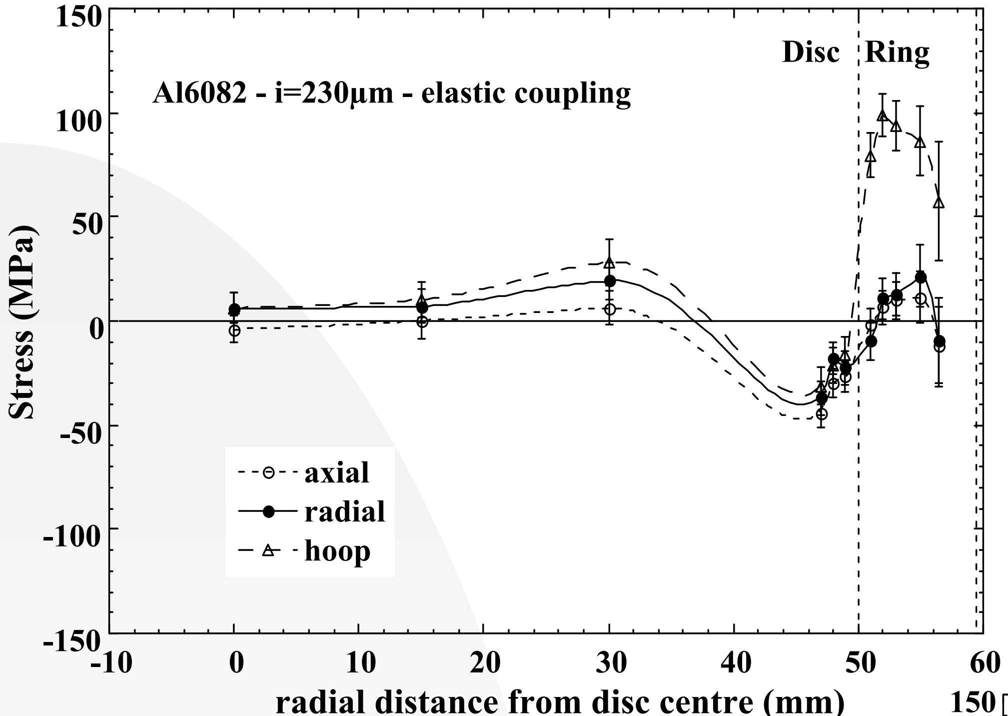

Good agreement with FEM calculations

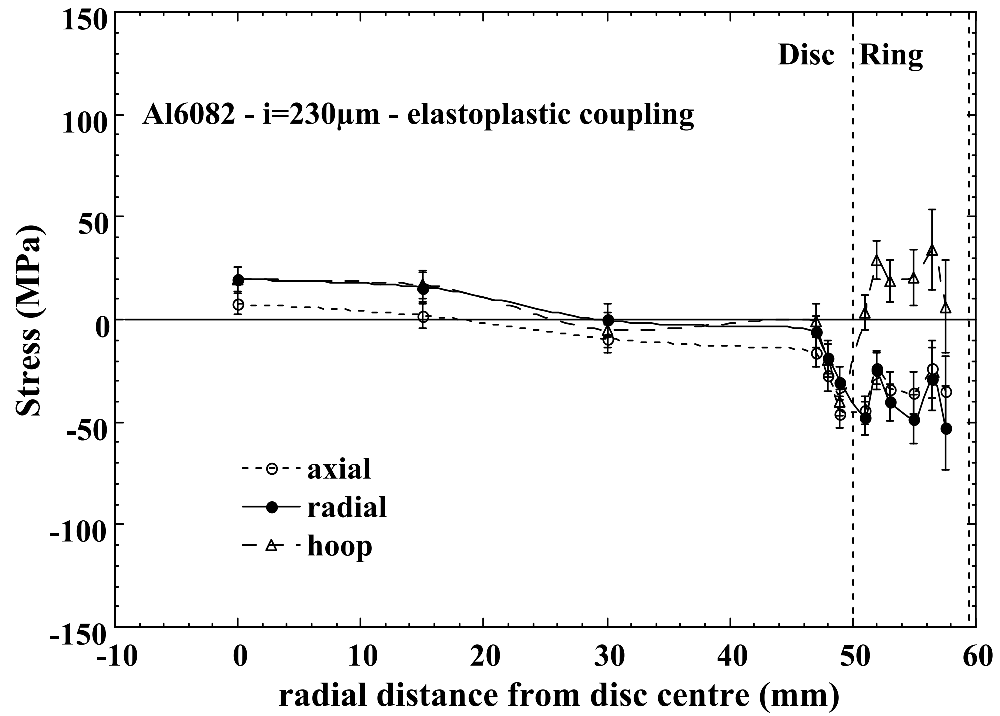

Neutron diffraction for residual stress determination

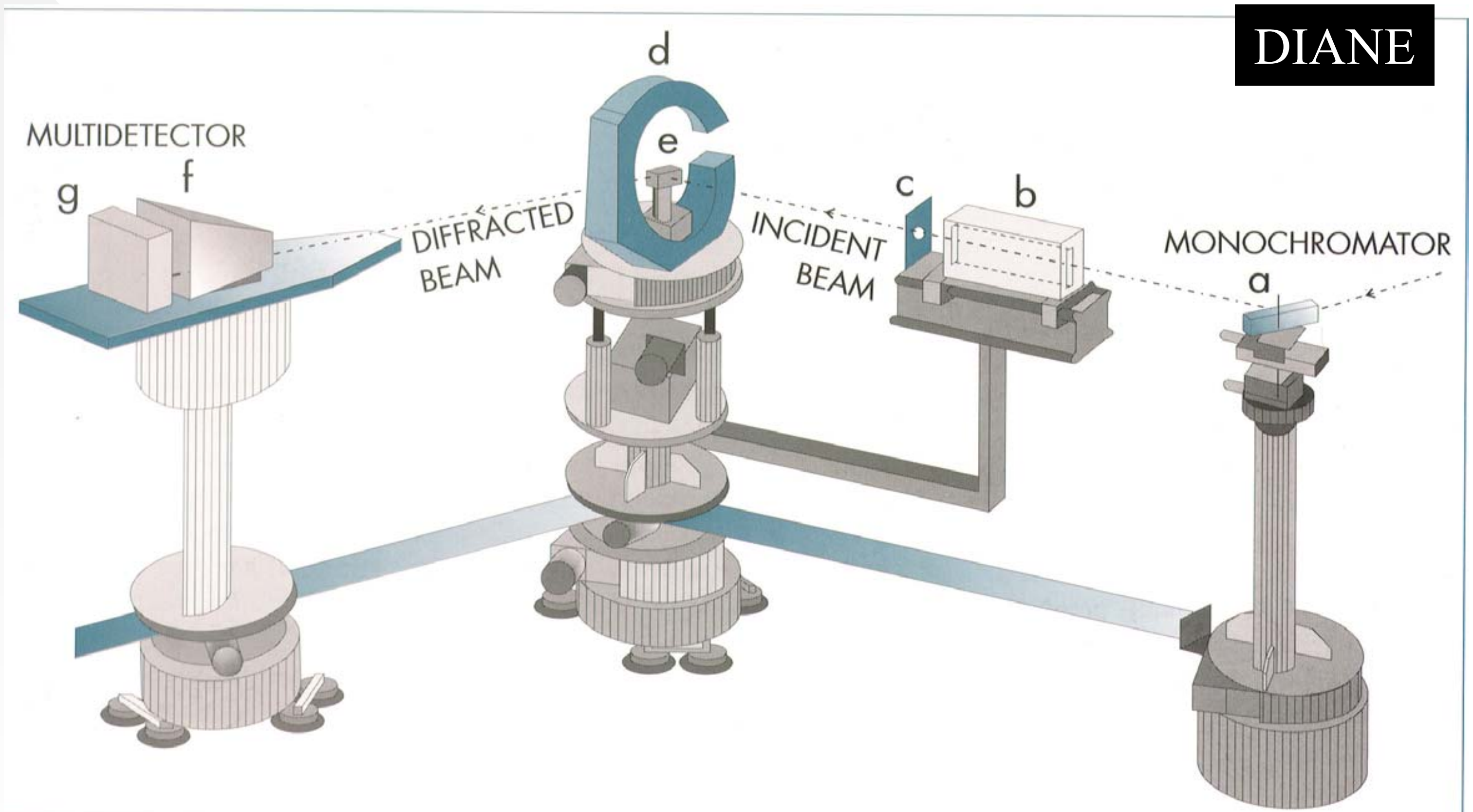

Residual stress measurements by neutron diffraction

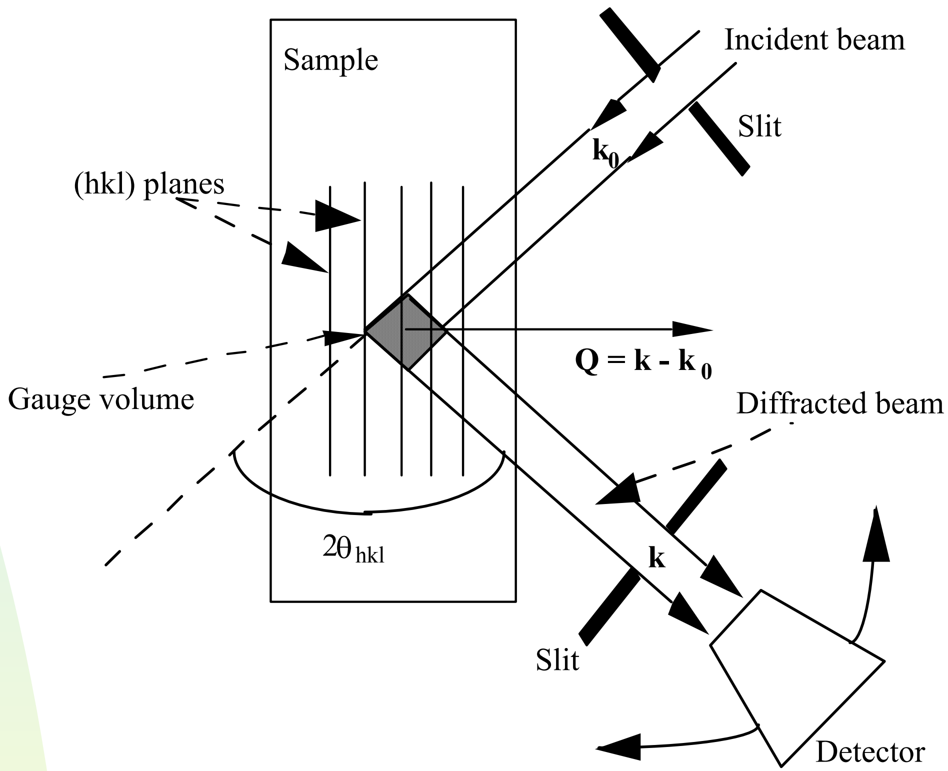

k_0 = wave vector of incident neutrons

k = wave vector of diffracted neutrons (|**k**| = |**k_0**|)

Q = **k** - **k_0** = scattering vector

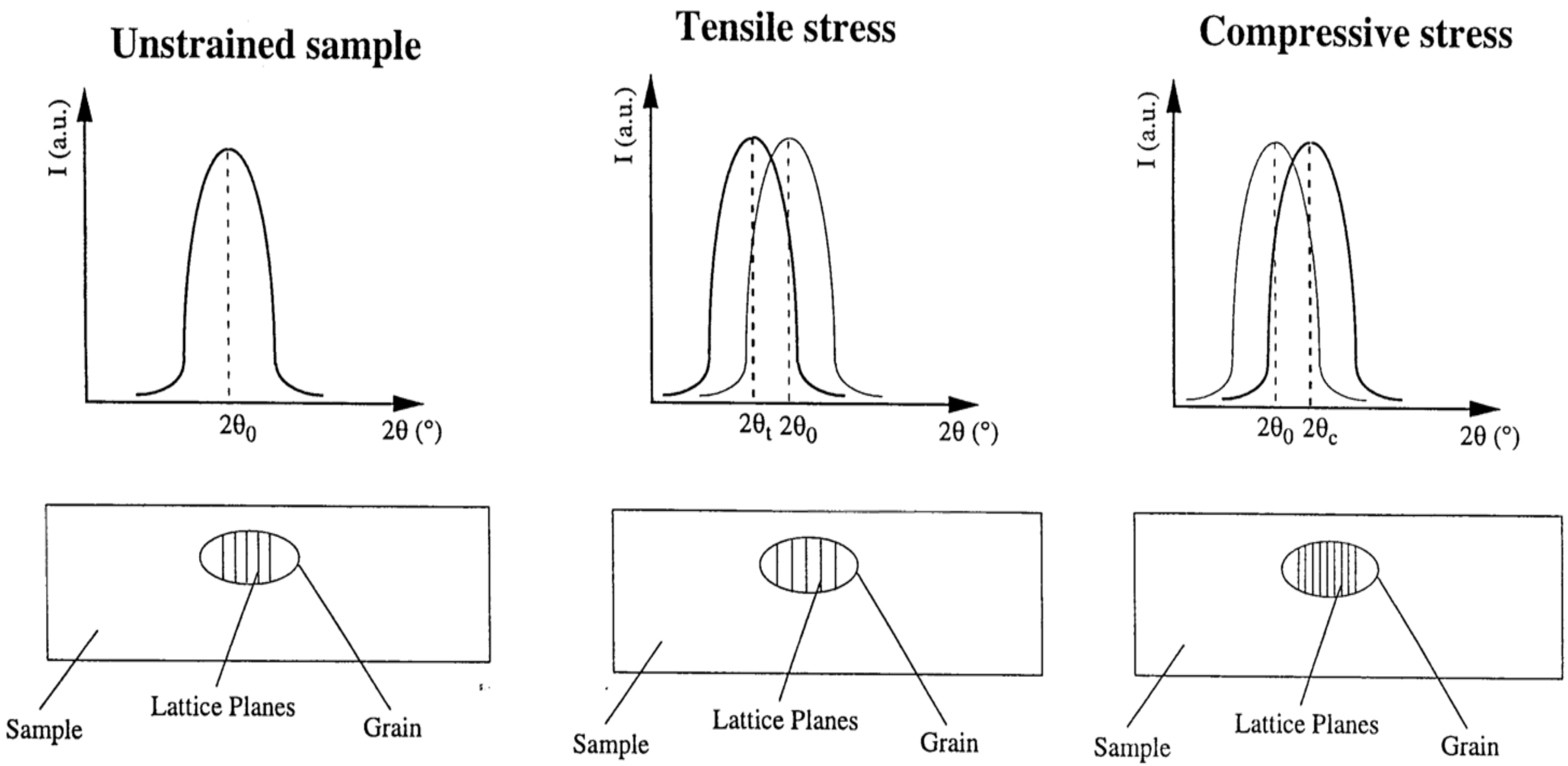

Bragg's Law: $\lambda = 2d_{hkl} \sin\theta_{hkl}$

(d_{hkl} = interplanar distance for hkl planes)

Strain: $\varepsilon = (d_{hkl} - d_{0,hkl}) / d_{0,hkl}$

(d_0 = "unstrained" interplanar distance)

- **Choose the (hkl) planes** to be investigated and adjust the neutron wavelength so that the Bragg's law is fullfilled for a given θ (usually $2\theta \approx 90°$ for the best definition of the gauge volume)

- **Determine the precise position of the Bragg peak** and then the interplanar distance d_{hkl} by the Bragg's law

- **Evaluate the strain** as

$$\varepsilon = \frac{d_{hkl} - d_{0hkl}}{d_{0hkl}}$$

where d_{0hkl} is the unstrained interplanar distance

- **Repeat the measurements in several spatial directions** to determine the six components of the strain tensor (only 3 directions if the principal strain axes are known)

- **Calculate stresses** by means of elasticity theory equations (Hooke's law)

Macro- and micro-stresses

- The macrostresses can be calculated from the measured stresses in both phases as follows:

$$\sigma_{macro} = f\ \sigma_{tot}^{Al_2O_3} + (1 - f)\sigma_{tot}^{Al}$$

where f is the volume fraction of the reinforcement.

- The microstresses (essentially thermal) in each phase are given by:

$$\sigma_{micro}^{i} = \sigma_{tot}^{i} - \sigma_{macro}$$

Follow-up of two European projects:

1) MISPOM " Development of models for the prediction of the in-service performance of MMC components" (contract.n.BRPR-CT97- 0396)

2) COFCOM "Computer assisted optimisation of the forming process of MMC Components" (contract.n.BRPT-CT97- 803).

Partners: Aerospatiale (F), Centro Ricerche Fiat - Teksid (I), Defence Evaluation and Research Agency (UK), Erich Schmid Institut (AT), Stampal - Simbi division (I), British Aluminium Speciality Extrusions (UK), INFM - University of Ancona (I), Universitat Politecnica de Catalunya (ES), National University of Ireland (IE), Eurocopter (F).